الجمهورية الجزائرية الديمقراطية الشعبية
People's Democratic Republic of Algeria
وزارة التعليم العالي و البحث العلمي
جامعة محمد خيضر بسكرة
University of Mohamed Khider BISKRA

Faculty of Exact sciences , natural and life sciences
Department of Material Sciences

العلوم الدقيقة وعلوم الطبيعة والحياة
قسم علوم المادة

Ref : ……

المرجع: ……

Thesis submitted for the award of the diploma of:

Science Doctor of Physics

Option: Materials physics

Entitled:

A new corrosion inhibition for protection of steel

Presented by :

Mr. Bouzid BOUAMRA

Soutenue : 04/07/2024

Committee members:

Okba BELAHSSEN	**Professor**	**President**	**University of Biskra**
Hamza BENTRAH	**Professor**	**Supervisor**	**University of Biskra**
Lazhar BOUHDJER	**MC-A**	**Examiner**	**University of Bouira**
Soufiane BENHAMIDA	**MC-A**	**Examiner**	**University of Ouergla**

Academic year: 2023/2024

Acknowledgements

This work was carried out at the Laboratory of Thin Films and Applications Physics (LPCMA) at the University of Biskra, as well as the Pedagogical Laboratory of Metallurgy in the Department of Mechanical Engineering at the University of Biskra.

First and foremost, I extend my deepest gratitude to Professor BENTRAH Hamza, my thesis supervisor, who skillfully guided my work while also granting me the freedom to make my own choices. I am thankful for his trust and availability despite his numerous responsibilities, as well as the valuable remarks and relevant advice he provided throughout this work.

A big thank you to Doctor DJELLAB Mounir. His active participation in in-depth discussions, insightful and honest critiques, enthusiasm, and encouragement have been crucial to me.

A special thank you to Mr. KHERIEF Slimane

I offer my sincere thanks to the jury members, Mr. Okba BELAHSSEN, Professor at the University of Biskra, Mr. Lazhar BOUHDJER, Doctor at the University of Bouira, Mrs. Soufiane BENHAMIDA, Doctor at the University of Ouargla, for the honor they bestowed upon me by agreeing to evaluate this work.

To all the professors from the universities of Laghouat , Oum El Bouaghi , Batna , Biskra , Tebessa , Jijel , Setif , Constantine, Ouargla, Eloued , Khenchela , and Ghardaia , who helped me, I extend my deepest thanks.

A special thanks to: T. Saoud , Y. Ferhi , K. Djail, M.H.Attia , M. Naoui ,O.Saoud ,W.Bouamra and K. Rezaiguia.

Finally, I am immensely grateful to my family,my wife S.ROUIBAH… my children Mouaadh, Amna ,Roufaida ,Sara , and all the people in my circle, friends, and close colleagues, who supported and accompanied me whenever I needed it.

Bouzid BOUAMRA

Dedication

I dedicate this humble work to everyone,

To my dear parents, may they rest in peace and may Allah grant them a place in His vast gardens,

To my small family, my beloved wife: S. Rouibah , and my dear children, Mouaadh , Amna, Roufaida , and Sara .

To my brothers and sisters, and to my extended family,

To all my teachers and everyone who taught me even a single letter, especially mentioning Professor Hamza Bentrah and Dr. Mounir Djellab, and not forgetting my dear professor during my master's, Miloud Sebais at the University of Constantine 1,

To all my colleagues, friends, and loved ones, and even my students,

To everyone who supported me on my journey, whether near or far.

Bouzid BOUAMRA

Contents

List of Figures

List of Tables

List of Abbreviations

Abbreviation	**Words refer to**
TM	thermomechanical
MIC	microbial-induced corrosion
SRB	sulfate-reducing bacteria
EFE	E.falcata extract
CPE	constant phase element
ASTM	The American Society for Testing and Materials
PARCOM	The Paris Commission
CEN	European Committee for Standardization
ISO	, International Organization for Standardization
AISI	*American Iron and Steel Institute*
API	*American Petroleum Institute*
PDP	Potentiodynamic polarization
EIS	Electrochemical impedance spectroscopy
OCP	Open-circuit potential
CMC	Carboxymethyl cellulose
AG	Arabinogalactan
GDE	Ghars date extract
Krd	Karkade

List of Equations

General Introduction

General Introduction

Corrosion has caused fractures in transport pipelines and oil leaks, leading to environmental pollution.[1] and severe economic losses.[2] Carbon steel has been widely used as a material for fabricating transmission pipelines.[3] Acids are used in various modern processes, such as cleaning, descaling, and pickling. In all these processes, carbon steel consistently corrodes.[4] Therefore, the use of corrosion inhibitors is inevitable. Depending on their nature, inhibitors can generally be categorized into two types: organic inhibitors and inorganic inhibitors. Inorganic inhibitors, such as nitrate-based and chromate-based inhibitors, are known to cause environmental pollution and are toxic.[5] Organic inhibitors can generally be classified into two types: natural organic inhibitors and synthetic organic inhibitors. Unfortunately, some synthetic organic inhibitors are non-biodegradable. [6]. Expensive, and hazardous.[7] Natural polysaccharides have proven to be effective corrosion inhibitors due to their easy availability, non-toxic nature, and biodegradability. Numerous studies have been published on the use of natural polysaccharides as corrosion inhibitors in acid solutions. For example, Abbout et al. used galactomannan, extracted from carob seeds, as a corrosion inhibitor for iron in a 1 M HCl solution. In the presence of 1 g/L galactomannan, the corrosion inhibition efficiency reached 87.72%.[8] Zhang et al. exploited Aloe polysaccharide as a corrosion inhibitor for mild steel in 15% HCl, and the inhibition efficiency was 96.41%.[9] Nwanoneny et al. confirmed an inhibition rate of 89.5% obtained with 5 $g.l^{-1}$ soy polymer for carbon steel in 1 M H_2SO_4.[10] However, research on the inhibition efficiency of natural polysaccharides for pipeline steel in acid solutions is still lacking. Reviews indicate that reported polysaccharides are generally less effective in sulfuric acid compared to hydrochloric acid for the corrosion inhibition of carbon steel. Xanthan gum, however, has been found to be an excellent corrosion inhibitor for mild steel in 15% hydrochloric acid, achieving 92% inhibition efficiency at 25°C.[11] Arabinogalactan (AG) from Tragacanth gum has proven to be an effective inhibitor for carbon steel in hydrochloric acid, achieving an inhibition efficiency of 96.3% at a concentration of 500 ppm AG.[12] The inhibition efficiency of Carboxymethyl cellulose (CMC) in sulphuric acid for mild steel was 64% at 0.5 $g.l^{-1}$ CMC.[13] The maximum inhibition efficiency of glycine max meal aqueous extract by infusion.[14] For carbon steel in 0.5 M sulfuric acid, arabinogalactan (AG) achieved an inhibition efficiency of 83.2% using the potentiodynamic polarization method. The inhibition efficiency of polymers can be synergistically enhanced by the addition of iodide

ions in the acidic medium.[15]Date palm (Phoenix dactylifera L.) comprises almost 2,500 species and around 200 genera. [16] Date palm fruits play a central role in the social and economic aspects of the world's arid and semi-desert climates. [17] Every variety of date palm fruit has a high content of polysaccharides. [18, 19] as well as high phenolic and flavonoid compounds. [20, 21] The principal phenolic compounds detected in date fruit include phenolic acids (such as 4-caffeoylshikimic, ferulic, vanillic, gallic, p-hydroxybenzoic, protocatechuic, p-coumaric, syringic, and caffeic acids), flavan-3-ols, proanthocyanidins, anthocyanins (such as cyanidin), and flavonoids (such as quercetin, luteolin, and apigenin).[22, 23] Studies have shown that some of these compounds (apigenin. [24] gallic acid. [25] and caffeic acid. [26]) have good inhibition efficacy in acidic media for carbon steel. Algeria produces 1,151,909 tons of dates. [27] Two cultivars are predominant in the local market with 96% (Deglet Nour and Ghars). [28]

The work presented in this thesis aims to evaluate the enhancement of corrosion inhibition of Ghars date extract (GDE) with iodide ions in a synergistic manner, for API5L X70 pipeline steel in 0.5M sulphuric acid by surface analyzes and electrochemical methods. The structure of this thesis reflects this approach.

Chapter I: is devoted to the bibliographic synthesis on the different inhibitors extracted from natural plants, which have allowed researchers to achieve high inhibitory efficiency values for steel in contact mainly with hydrochloric and sulfuric acid.

Chaptre II: briefly explain all the experimental techniques used in this study as well as the experimental conditions adopted.

All the results are grouped in chapter III. The third chapter included the following points: the study of the FTIR spectra of GDE to determine the functional group of the inhibitor, the optimization of GDE concentrations for 0.5 M H_2SO_4 , the synergistic effect of the GDE with iodide ions, and finely the proposed mechanism of corrosion inhibition of GDE/iodide ions system.

CHAPTER I

BACKGROUND AND LITERATURE REVIEW

I.1.Corrosion of carbon steel API 5L X70 in acidic media for the oil and gas industry

Carbon steel is the most frequent material used for transmission pipes in the gas and oil industries, and it can withstand a variety of corrosive situations. Sulfuric acid is used in a variety of service contexts, including pickling, boiler cleaning, de-scaling, and oil well acidification. [29,30]

In the petroleum industry, carbon steel is the most commonly used material in piping, both upstream and downstream. As such, carbon steel is an important material due to its good mechanical performance and relatively low cost compared to higher alloy materials. [31] In addition, the corrosion resistance of these materials is poor, meaning that engineering products have a shorter lifetime and less performance. Therefore, methodologies are required that inhibit corrosion. [32]

Corrosion problems occur in the petroleum industry in at least three general areas [33]:

1- Production.

2- Transportation and storage.

3- Refinery operations.

Pipelines used to carry natural resources such as oil and gas are installed in a variety of service conditions, some of which create great issues due to severe environmental deterioration and ultimate collapse, resulting in significant losses. [34] The pipeline sector has seen an increase in demand for larger pipe diameters, higher operating pressures, and a greater variety of materials conveyed. To avoid huge wall thicknesses, greater strength steel types are used. [35] High strength X70 grade steel (marking a minimum yield strength of 70.3 psi/483 MPa) was introduced to the pipeline sector over 30 years ago, coinciding with the advent of thermomechanical (TM) rolling procedures. [36]

Current pipeline materials on the global market are frequently controlled in accordance with API standard 5L. API-5L's key design concerns are centered on alloy chemistry and tensile strength. The chemical compositions of X-grade steels are rather straightforward, with maximum restrictions on C, Mn ,S, P, and additional elements such as niobium and vanadium [37]. Despite their weak corrosion resistance, carbon steels are commonly employed in the oil and gas sector. these materials are favored over others due to cost concerns and the fact that corrosion generally results in widespread attack. API 5L

pipe steel is a low carbon steel utilized in the construction of transmission pipelines. [38, 39] The development of thermo-mechanical technology for high strength pipeline steels such as X-80, X-100, and X-120 allowed for a reduction in wall thickness and, in certain cases, an improvement in corrosion resistance. [40, 41] However, because the API 5L pipe is still prone to water corrosion, inhibitor addition is a common corrosion control method. Imidazoline inhibitors have been used for over 45 years with improving results. [42, 43]

I.1.1. Corrosion Mechanism in Acidic Medium

The most common form of corrosion in the oil and gas industry occurs when steel comes in contact with an aqueous environment and rusts. When metal is exposed to a corrosive solution (the electrolyte), the metal atoms at the anode site lose electrons, and these electrons are then absorbed by other metal atoms at the cathode site. The cathode, in contact with the anode via the electrolyte, conducts this exchange in an attempt to balance their positive and negative charges. Positively charged ions are released into the electrolyte capable of bonding with other groups of atoms that are negatively charged.

The figure I-1 shows the corrosion process:

Anodic Reaction (Oxidation):

$$Fe \rightarrow Fe^{2+} + 2e^- \qquad \textit{Equ I- 1}$$

Cathodic Reaction (Reduction):

$$2H^+ + 2e^- \rightarrow H_2 \qquad \textit{Equ I- 2}$$

Global Reaction (Oxydo/Reduction):

$$Fe + 2H^+ \rightarrow Fe^{2+} + H_2 \qquad \textit{Equ I- 3}$$

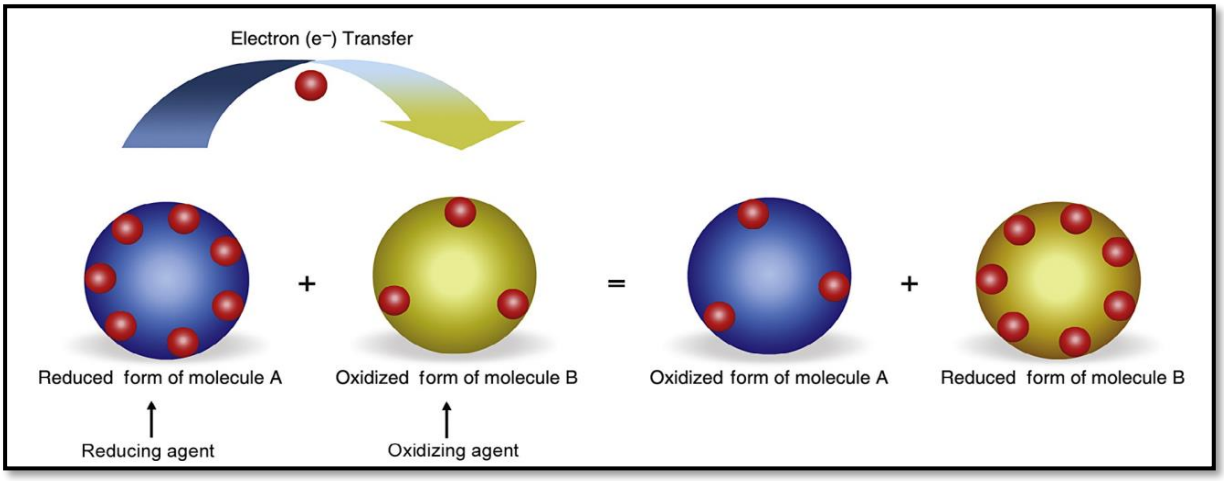

Figure I. 1: A full oxidation-reduction reaction involves the transfer of electrons from one species (the reducing agent) to another (the oxidizing agent). [44]

I.1.2. Types of corrosion of carbon steel API 5L X70

Corrosion types according to ASM (2000), corrosion may be characterized based on three factors: the composition of the corrodent, the process of corrosion, and the look of the damaged metal. [45]

In acidic environments, generalized corrosion is the most common form for carbon steels. However, in the presence of metallic oxidants such as Fe^{3+} and Fe^{2+}, localized pitting corrosion occurs.

Ferric ion (Fe^{3+}) is responsible for both generalized corrosion and pitting corrosion of carbon steels. [46] and the detrimental effect is exacerbated in the presence of hydrochloric acid (with Cl^- ions). Corrosion occurs when there is a precipitation of iron oxides with aeration during the acid cleaning procedure. [47]

Corrosion is often regarded as an abiotic process controlled by electrochemical or physicochemical processes. [48]

Figure I. 2.The main forms of corrosion. [49]

I.1.1.1. Uniform corrosion

As mentioned, is equally dispersed throughout the metal surface. anodic and cathodic zones are present and may generally shift from one spot to the next as corrosion progresses. [50] In most circumstances, the corrosion rate slows with time and eventually approaches a steady state value. The presence of corrosion products, which create a semi-protective coating on the metal surface, regulates this. During the corrosion process, the layer functions as a diffusion barrier past which metal ions and oxygen must pass.

I.1.1.2. Pitting corrosion

Pitting occurs at localized areas of the metal surface and may lead to rapid penetration of a barrier. The mechanism is caused by the perforation of a "passive," usually

oxide, film on the metal. This region becomes anodic while the large area of material around this site is cathodic. after pit initiation, the anodic and cathodic areas remain in place. The large cathodic area results in rapid metal dissolution in the pit. Chloride in seawater is a major factor in the breakdown of passivity in a metal surface. As chloride concentrates in the pit the PH decreases, causing an initial increase in the rate of attack in the pit. [51,52] The rate of pit development slows when the pits fill with corrosion products.

It has been discovered that the depth of the hole is frequently related to the thickness of the evenly corroded layer. As a result, a "pitting factor" has been defined as the ratio of maximum pit depth to average uniform corrosion penetration as assessed by descaled weight loss measurements. [53] Metals with a high pitting factor are obviously not good alternatives for saltwater service.

I.1.2.Oxidizing agents

The two main oxidizing agents encountered in practice are : [54]

- Solvated protons (H^+)
- Dissolved oxygen (O_2)

However, other oxidants can also corrode metals, such as : [54]

- Oxidizing metal cations: Cu^{2+}, Fe^{2+}, Fe^{3+}, Sn^{2+}
- Oxidizing anions: NO_2^-, NO_3^-, $Cr_2O_7^{2-}$, MnO_4^-, ClO^-
- Dissolved oxidizing gases: O_3, CO_2, SO_3

I.1.3. Oil well stimulation

I.1.3.1. Acid injection

Acidizing is the process of injecting acid into a damaged wellbore or other damaged formation that can yield oil and gas. this operation is intended to improve the well's productivity or injectivity through the acid’s ability to dissolve depositions of minerals. [55]

Damaged wells are those which suffer a restriction in flow rate. This may be due to a number of causes, for example, drilling damage or build-up of carbonate scale. Damage may occur at the wellbore face or as a zone of reduced permeability extending several inches or even feet into the formation which severely restricts productivity. If the damage

can be removed, very significant increases in production rate can be achieved. [56] There are three general categories of acid treatments:

A- In acid washing: the objective is simply tubular and wellbore cleaning. treatment of the formation is not intended. Acid washing is most commonly performed with hydrochloric acid (HCl) mixtures to clean out the scale (such as calcium carbonate), rust, and other debris restricting flow in the well. [57]

B- Matrix acidizing: the process involves the injection of acid mixtures below the fracture pressures of rocks near the wellbore. Its purpose is dissolving sediments to reinforce rock permeability and the establishment of a clean zone within the reservoir, thus eliminating the restrictions for oil flux into the wellbore zone. Commonly, matrix acidizing is applied in case of tighter carbonate and sandstone formations, it is recommended in the industry to utilize acids with mass concentrations, in the range of 10–15%. [57]

C- Fracture acidizing: is implemented in case of carbonate formations with relatively higher acid mass concentrations, in the range of 20–30%. This method involves acid injection above the fracture pressures of rocks near the wellbore to create channels or so-called wormholes, as the resulting rock fractures, under pressure from the hydrocarbons, might immigrate through. [57]

I.1.3.2. The main stages of acidizing

A- Pre-flush stage is employed to dissolve any Na, K, and Ca ions that may produce insoluble silicates when reacted with the silica. besides preventing the live HF acid to enter into a high pH region, pre-flush also provides a low pH region reducing the risk of precipitate formation. [58]

B- Main acid stage is applied to dissolve the quartz, clay, feldspar and silicates. This acid may also dissolve the remains of carbonates present after the pre-flush stage. [58]

C- After-flush stage is used to keep the wettability of the formation to the original state and it cleans the formation rapidly by removing the spent acid. Mutual solvents, diesel oil, NH_4Cl , acetic acid, or HCl can be applied at this stage for the efficient displacement of the spent acids. [58]

I.2.Protection of carbone steel against corrosion in acidic media by corrosion inhibitors

Among the methods to avoid or prevent the destruction or degradation of metal surfaces, the corrosion inhibitors are one of the best know methods of corrosion protection and one of the most useful in the industry. This method is following stand up due to its low cost and practice method. [59]

I.2.1. Organic inhibitors

Organic corrosion inhibitors are a class of molecules that delay or minimize the corrosive process. It has been shown that their effectiveness is mainly related to adsorption on the metal surface, acting as a barrier layer and reducing aggressive species access, usually, they get adsorbed on the metal surface by displacing water molecules, and the bonding efficiency is enhanced by the presence of polar functions with S, O, or N atoms in the molecule, heterocyclic compounds, and electrons. [60]

A.Hamdy and Nour sh. El-Gendy. [61] Studied the corrosion inhibition of carbon steel by *Henna* extract in acid medium, in a 1 M HCl solution. henna extract inhibits the corrosion of carbon steel. The effectiveness of inhibition improves with increasing inhibitor concentration but decreases with rising temperature also the apparent activation energy values rise as the inhibitor concentration increases. The activation enthalpy illustrates the endothermic character of the carbon steel dissolving process. The entropy of activation rises with increasing inhibitor concentration, resulting in an increase in system disorder. The Langmuir adsorption isotherm is followed by henna extract adsorption on carbon steel. The adsorption process is spontaneous and endothermic, as indicated by Gibb's free energy, enthalpy, and entropy of adsorption, and the inhibitor molecules are adsorbed on the metal surface by physical adsorption. The results of polarization measurements. The polarization tests demonstrated that *Henna* extract operates as a mixed sort of inhibitor. The corrosion of carbon steel in 1 M HCl is confirmed by EDX and SEM, and it is inhibited by *Henna* extract. FTIR and XRD demonstrate that the chemicals included in the plant extract form a corrosion inhibitive layer by complexing with iron ions on the carbon steel surface. The inhibitor can be deposited on the metal surface via the oxygen atom of lawsone, which is the primary ingredient of *Henna* extract.

The inhibition action of aqueous *Coffee* ground extracts on the corrosion of carbon steel in HCl solution was studied by Vanessa Vasconcelos et al. [62] In a 1 mol L^{-1} HCl solution, aqueous extracts of *Coffee* grounds can operate as an efficient, naturally

generated green corrosion inhibitor for carbon steel. All electrochemical results, including slightly lower values for OCP and corrosion potential, indications of inhibitory action in the anodic and cathodic polarisation curves, and electrochemical impedance measurements, demonstrated that the extracts tested acted as mixed-type inhibitors with a cathodic bias. The adsorption of the studied extracts was consistent with the Langmuir adsorption isotherm. the inhibitory effectiveness of carbon steel in 1 $mol.L^{-1}$ HCl increased with increasing temperature, when the extract was employed, the apparent activation energy (Ea) of carbon steel dissolving reduced. A strong chemisorptive bond is responsible for the extract's effect as a corrosion inhibitor for carbon steel in acid solution. The minor changes in chlorogenic acid composition and total phenolic contents seen between the two *Coffee* extracts are compatible with the minor differences in inhibitory effectiveness reported between the two extracts. The presence of isolated chlorogenic acids does not appear to explain the observed corrosion inhibition in *Coffee* extracts. It is unclear to say what components in the *Coffee* extracts generated their comparatively high capacity to stop corrosion in this investigation.

A.El Bribri et al. [63] Identified the use of *Euphorbia falcata* extract as eco-friendly corrosion inhibitor of carbon steel in hydrochloric acid solution. The *E.falcata* extract (EFE) has strong inhibitory characteristics for carbon steel corrosion in 1 M HCl solutions at 30 °C. As expected, the corrosion inhibition effectiveness improves with EFE concentration, with a maximum inhibition efficiency ɳ (%) of nearly 93% at 3.0 $g.L^{-1}$. The corrosion inhibition efficiencies determined by weight loss, electrochemical impedance spectroscopy (EIS) and potentiodynamic polarization method are quite consistent.

A relatively basic structural model with only one time constant adequately describes the EIS spectrum. It is made up of a charge transfer resistance Rt in tandem with a double-layer capacitance that is dispersed and so described by a constant phase element (CPE). With increasing EFE concentration, the computed structural parameters demonstrate an increase in the derived Rt values and a reduction in the capacitance, Cdl. This behavior is thought to be caused by an increase in the thickness of the adsorption layer at the steel surface. Tafel polarization results demonstrate that in 1 M HCl media, EFE works as a mixed-type inhibitor. The Langmuir adsorption isotherm accurately describes the adsorption of *E.Falcata* extract (EFE), and the computed value of ($\Delta G°ads$) indicates that the adsorption mechanism of this substance on carbon steel surface in 1 M HCl solution is mostly due to physisorption.

Hicham Taoui et al. [64] Used Bark resin of Schinus molle as an eco-friendly inhibitor for API 5L X70 pipeline steel in HCl medium. according to FTIR study, BRSM comprises O and maybe N atoms in functional groups (O-H, N-H, C=O (ketone), C-N, C-O) and aromatic ring. The effectiveness of inhibition rises with inhibitor concentration, reaching a maximum of 94% at 2 $g.L^{-1}$.

The Langmuir adsorption isotherm was found to provide the best explanation of the inhibitor adsorption behavior. Also, the adsorption of BRSM may be described by two types of interactions: physical adsorption and chemisorption. Because of the acquired value of ΔG_{ads}, the physisorption mode is more likely to prevail, and the potentiostatic polarization results show that the inhibitor impacts both cathodic and anodic processes, indicating that it is a mixed type. The results of polarization and EIS tests indicate that the geometric blocking action of BRSM is the mode of inhibition. According to the findings of the EIS research, the corrosion of API 5L X70 pipeline steel in the presence of BRSM is mostly regulated by the charge transfer mechanism.

The corrosion resistance of carbon steel in weak acid solutions in the presence of **L**-histidine as corrosion inhibitor was investigated by Marian Bobina et al. [65] L-histidine is a mixed safe corrosion inhibitor for carbon steel in mild acid solutions that acts on the cathodic process of hydrogen evolution as well as the anodic process of metal dissolution. Three independent approaches were used to measure inhibition efficiency: weight loss, linear polarization, and electrochemical impedance, all of which produced equivalent findings. the efficiency of inhibition improves with the quantity of inhibitor used, with 10^{-2} M L-histidine achieving the highest value of 81.6%. The Langmuir isotherm governs amino acid adsorption on metal surfaces, and the Gibbs free energy value reveals the electrostatic interactions between charged molecules and charged carbon steel. In general, free energy values smaller than -40 kJ mol^{-1} are linked with processes involving physical adsorption of the inhibitor on the metal surface. It prevents corrosive media from penetrating. The double layer capacitance derived from EIS tests diminishes as inhibitor concentration increases, implying an adsorption process of L-histidine on the metal surface. L-high histidine's inhibition efficiency in acetic acid/sodium acetate solutions make it a viable option as an environmentally acceptable corrosion inhibitor in deicing solutions containing sodium acetate. the benefits of this inhibitor include biodegradability and low environmental effect.

Ahmed Abdel Nazeer et al. [66] focused on the corrosion inhibition of carbon steel by *Roselle* extract in hydrochloric acid solution: electrochemical and surface study, as a result, in 0.5 M HCl solution, *Krd* proven to be a more efficient corrosion inhibitor for carbon steel. This green inhibitor is a hybrid inhibitor. The EFM approach was shown to be more efficient when the concentration was increased to 91.0% in the presence of 500 ppm Krd extract at 25 °C and less efficient when the temperature was increased to 55 °C at 87.6%. *Krd* was shown to obey the Langmuir adsorption isotherm when inhibiting carbon steel in 0.5 M HCl solution. The thermodynamic values provided from this work show that the presence of this inhibitor raises the activation energy, with negative ΔG_{ads} suggesting spontaneous adsorption of the inhibitor on the steel surface. The results of the EIS, EFM, and potentiodynamic polarization measurements match well with the SEM/EDX data.

I.2.2. Inorganic inhibitors

Inorganic inhibitors such as dichromates, chromates, tungstates, molybdates, nitrites, and nitrates have been used as corrosion inhibitors. These inhibitors are powerful oxidizing agents. They have other important roles such as chelating agent and abrasive particle. The effectiveness of some corrosion inhibitors depends upon the type of material, its properties and the corrosion environment. For instance, inhibition efficiency of molybdate anion increases with the increasing of oxygen concentration in a corrosion environment. Some of these anions have been used satisfactorily in many corrosive environments. For example, molybdates have been used to prevent mild steel corrosion, on bacterial corrosion. Nitrates have been used to prevent galvanized steel, and zinc corrosion in NaCl solution. Chromates are a very effective corrosion inhibitors for iron and ferrous alloys in the presence of halide ions. [67]

I.2.3. Inhibition mechanism of organic inhibitors

When metals come in close contact with aggressive media, their surfaces corrode. The speed and extent of the corrosion process depends on several factors like concentration of the aggressive medium and temperature. Corrosion inhibitors have been employed extensively to control corrosion of metals in various aggressive media. It is generally believed that a given corrosion inhibitor functions by adsorption on metal surface and formation of thin protective films or layers that blanket the metal surface from the aggressive medium. The nature of interaction between the film formed and the metal surface may be explained with the help of adsorption isotherms. Adsorption involves adhesion (or concentration) of atoms, molecules or ions on the surface of a substance, most

often, a solid. The surface to which the molecule or atom is adhering is called the adsorbent while the molecule or atom itself is called the adsorbate. Therefore, the adsorption phenomenon is essentially an attraction of adsorbate species on the adsorbent surface. The preferential concentration of adsorbate molecules in the proximity of the adsorbent surface arises from the unsaturated nature of surface forces of the adsorbent. Verma et al. [68] Opines that adsorption of corrosion inhibitors may be seen as a substitution process where the inhibitor molecules in the aqueous phase replace water molecules already adsorbed on metal surface. The mechanism by which adsorption takes place may be physical or chemical in nature, also referred to as physisorption or chemisorption respectively .

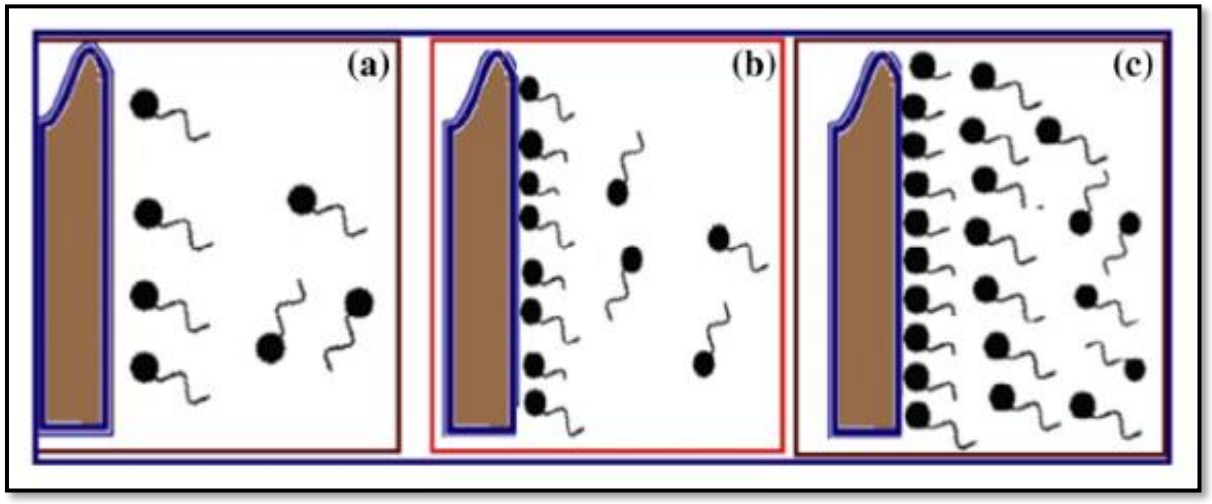

Figure I. 3: Inhibitor adsorption on mild steel surface. (a) Adsorption in the presence of inhibitor at a low concentration. (b) Adsorption in the presence of inhibitor at a high concentration. (c) Adsorption in the presence of inhibitor at a higher concentration. [69]

I.2.4. Adsorption of organic inhibitor

Adsorption is the selective transfer of certain components of a fluid phase, called solutes to the surface of an insoluble solid. The adsorbed solutes are referred to as adsorbates, and the solid material as adsorbent. When an adsorbent is exposed to a fluid phase, molecules in the fluid phase diffuse to its surface, where they are either chemically bond with the solid surface or are held there physically by weak van der Waals intermolecular forces. When adsorption is caused by Van der Waals forces, it is referred to as physical adsorption or physisorption, whereas it is called chemical adsorption or chemisorption if it is caused by chemical forces. [70]

I.2.4.1. Physical adsorption

As result of the bonds that those atoms have with the neighboring atoms of the same substance. Adsorption is carried out on such surfaces through natural attractive forces or the so-called vander waals forces. This type of adsorption can be in the form of multiple layers of the adsorbent material on the surface of the adsorbent material when suitable conditions of pressure and temperature are available. The adsorbent and the adsorbent, which is estimated at less than (20 kj.mol^{-1}), therefore, this type of adsorption does not need high temperatures and does not require activation energy and occurs at low temperatures similar to the process of condensation of vapors on the surfaces of liquid materials. [71]

I.2.4.2. Chemical adsorption

This type of adsorption occurs on surfaces that are not electronically unsaturated, as such surfaces tend to form chemical bonds with the atoms or molecules that have been adsorbed. As a first step in the chemical reaction that occurs between the adsorbent surface and the adsorbent material, this type of adsorption needs a high activation energy, as well as the accompanying temperatures are high and estimated in a quantity greater than (20 kj.mol^{-1}), and this type of adsorption is specific and is not reversed and limited by its layer Oxygen adsorption on coal surface, hydrogen chloride adsorption on iron surface.[71]

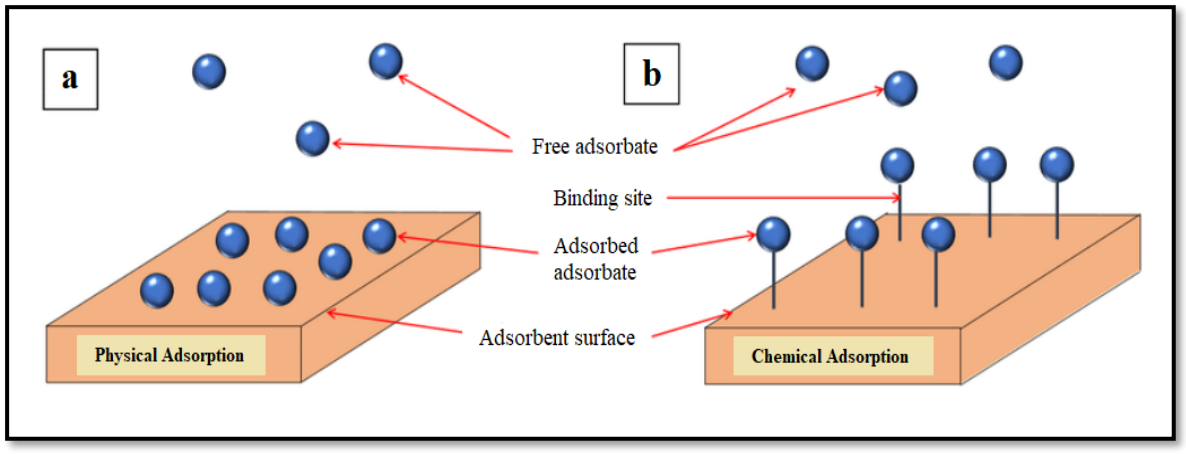

Figure I. 4: The mechanism of (a) Physical and (b) Chemical adsorption. [72]

In the table I.1. Chaouiki, A et al [73].summarizes the different properties between chemisorptiona and physisorption.

Table I. 1.Chemisoption and physisorption properties[73]

Physisorption : physical adsorption	***Chemisorption : chemical adsorption***
-Low heat adsorption usually< 20kj.mol^{-1}	-High heat adsorption usually> 20 kj.mol^{-1}
-Force of attraction are Van der waal's forces	-Force of attraction are chemical bond forces
-It usually takes place at low temperature and decreases with increasing temperature	-It takes place at high temperature
-It is reversible	-It is irreversible
-It is related to the ease liquification of the gas	-The extent of adsorption is generally not related to liquification of the gas
-It is not very specific	-It is highly specific
-It forms multi-molecular layers	-It forms mono-molecular layers
-It does not require any activation energy	-It requires activation energy

1.2.1.1. Synthetic organic inhibitors for steel in acidic media

The use of synthetic corrosion inhibitors is the most popular and effective method due to their association with cost-effective synthesis, high effectiveness and ease of application. the effectiveness of these organic inhibitors is based on the fact that generally they contain several heteroatoms in the form of polar functional groups such as –OH, NO_2, -OCH_3, - COOH, -NH_2, - $COOC_2H_5$, -$CONH_2$, etc . [74]

1.2.1.2. Natural organic inhibitor for steel in acidic media

Organic corrosion inhibitors are a class of molecules that delay or minimize the corrosive process. It has been shown that their effectiveness is mainly related to adsorption on the metal surface, acting as a barrier layer and reducing aggressive species access, usually, they get adsorbed on the metal surface by displacing water molecules, and the bonding efficiency is enhanced by the presence of polar functions with S, O, or N atoms in the molecule, heterocyclic compounds, and electrons. [75]

A. Organic polymers

The use of polymers as corrosion inhibitors has attracted considerable attention recently. Polymers are used as corrosion inhibitors because, through their functional groups they form complexes with metal ions and on the metal surface these complexes occupy a large

surface area, thereby blanketing the surface and protecting the metal from corrosive agents present in the solution. The inhibitive power of these polymers is related structurally to the cyclic rings, heteroatom (oxygen and nitrogen) that are the major active centers of adsorption. Polymers found in nature have shown promising results as metal corrosion inhibitors in different corrosive environments. [76]

I.Nadi et al.[77] Studied the inhibition effect of the invasive brown *Seawee Sargassum Muticum* extract (ESM),harvested from the atlantic coast of morocco, against the corrosion of carbon steel in 1 M HCl medium was studied for the first time using gravimetric, electrochemical and surface techniques. The methanolic crude extract of *Sargassum Muticum* (ESM) is rich in alginate biopolymer. The evaluation corrosion tests showed that this algal extract acts as a good mixed corrosion inhibitor for carbon steel substrate in 1 M HCl since inhibition efficiency of 97 % was reached with 1 $g.L^{-1}$ of ESM at 303 K. AC impedance findings showed that the seaweed extract adding in the corrosive electrolyte increases the polarization resistance and conversely decreases the charge capacitance at the interface.

Adsorption of ESM on the substrate surface followed the Langmuir adsorption isotherm. X-ray photoelectron spectroscopy analyses (XPS) demonstrated that the corrosion inhibition mechanism of carbon steel substrate in 1 M HCl environment by the investigated algal extract is typical of the chemisorption process and the protective barrier is mainly formed by the adsorbed biological macromolecules.

B. Organic pigments

Organic pigments are made up of carbon chains and rings. They may also comprise inorganic components to assist stabilize the organic component's characteristics. As an additional mode of protection, most organic corrosion inhibitory pigments can form closely packed complexes with the substrate, therefore blocking active sites. [78]

Lingjie Lia et al.[79] Studied the adsorption and corrosion inhibition of *Osmanthus Fragran* Leaves extract (OFLE) on carbon steel. They found that OFLE is a highly effective mixed inhibitor of carbon steel corrosion in 1 M HCl solution. And the adsorption of it on the surface of carbon steel follows the Langmuir adsorption isotherm and is a spontaneous, exothermic process with an increase in entropy. In addition, the AFM and FTIR data show the presence of a homogeneous and dense adsorptive coating across the carbon steel surface, which effectively prevents corrosion, and quantum-chemical

simulations of characteristics linked with the electronic structures of individual OFLE components confirm the inhibitory properties of OFLE to carbon steel corrosion.

M. Messali et al.[80] Investigated the Guar gum as a water-soluble, nonionic, nontoxic, biodegradable and biocompatible hetero polysaccharide with unlimited number of industrial applications. In this study, guar gum was evaluated as a natural inhibitor of carbon steel corrosion in 2 M H_3PO_4 solution. The characteristic effect of guar gum on the steel corrosion was studied at concentration ranges from 0.1 to 1.0 $g.L^{-1}$ at 298 to 328 K by weight loss and electrochemical methods. Obtained results showed that, the inhibition efficiency (η%) of guar gum decreased slightly when the temperature increased and increased by increasing the inhibitor concentration reaching the maximum value at 1.0 $g.L^{1}$.

The adsorption of guar gum on steel surface was studied by the Temkin adsorption model. EIS measurements indicate that the values of the polarization resistance (Rp) of CS in presence of guar gum are significantly higher than that of the untreated surface. Steel surface coated with guar gum was analyzed by SEM, FTIR and XRD.

C. Drugs and dyes

It has been considered to be more important and desirable for researchers to focus on the development of effective corrosion inhibitors of natural origin with non-toxic effects, in this context, drugs (chemical medicine) having its natural origin, with less harmful impacts on the human and aquatic environment, as well as their environmentally friendly characteristics, have been found to be one of the best contenders to replace the commonly used toxic corrosion inhibitors. [81] The presence of carbocyclic and heterocyclic systems, five and six-membered rings of aromatic compounds, commercially available drugs have also attracted much attention as green corrosion inhibitors

Researchers investigated the applications of dyes such as azo compounds methyl yellow, methyl orange, methyl red and alizarin yellow GG dye. [82, 83] As green inhibitors inhibition of mild steel in acidic media has been reported. [84,85] Mixed type inhibitor with predominant cathodic effect. Corrosion inhibition mechanism accomplished as the green dye molecules possess aromatic rings, electro-active nitrogen, and oxygen atoms, favoring the adsorption of dye molecules on the metal surface. In addition, dye molecules having large and flat structure occupying a larger area of the metal surface and thereby developing a protective coating.

Apart from the non-toxicity and biodegradable nature of various plants, dyes, drugs etc, The main problem lies with their cost and industrial scale production. They should be optimized on the basis of their availability and processing methods, so that they must be evaluated from an economical point of view before being used in industries.

I.3. Eco-friendly inhibitors for carbon steel in acidic media

The term "green inhibitor" or "eco-friendly inhibitor" refers to the substances that have biocompatibility in nature. The inhibitors like plant extracts presumably possess biocompatibility due to their biological origin. Similar to the general classification of "inhibitors", "green inhibitors" can also be grouped into two categories, namely organic green inhibitors and inorganic green inhibitors. [86]

I.3.1. Use of natural organic compounds as corrosion inhibitors for carbon steel in acidic media

H.Elabbasy et al. [87] Studied the inhibition effect of *Ambrosia Maritima*,which was also named after (*Damsissa*) extract, towards the corrosion of carbon steelin 1M HCl solution was investigated utilizing potentiodynamic polarization,electrochemical impedance spectroscopy (EIS) and electrochemical frequency modulation (EFM) methods. The process of adsorption obeyed Langmuir adsorption isotherm. *Damsissa* extract was found to act as a mixed-type in 1M HCl. The computed adsorption thermodynamic parameters demonstrated that the adsorption was a spontaneous, endothermic process accompanied by an increase in the entropy. The maximum value of the inhibition approached 92.6% within the presence of 300 ppm *Damsissa* extract utilizing Tafel polarization procedure. The results obtained from the various electrochemical processes were in a great agreement.The inhibition of the extract was assumed to occur through the adsorption of active ingredients on the metal surface. morphology of the surface was analyzed utilizing scanning electron.

Microscopy (SEM), Fourier transforms infrared (FTIR) and atomic force microscopy (AFM) which confirmed the presence of a protective film of extract molecule on carbon steel surface.

Subhadra Garai et al. [88] The search frameworks seized about comprehensive study on crude methanolic extract of *Artemisia pallens* (asteraceae) and its active component as effective corrosion inhibitors of mild steel in acid solution .

Based on the weight loss results, the corrosion inhibition efficacy of *Psidium Guajava* extract increases with increasing inhibitor concentration and declines with rising temperature. Thermodynamic investigation demonstrates the spontaneity of the inhibitor adsorption response on the metal surface. The linearity of the curve plotted between logC and clearly indicates the increasing adsorption of inhibitor on the metal surface as its concentration increases. As demonstrated by the results, the adsorption might be related to the lone pair of electrons present in the hetero atoms of the *Psidium Guajava* extract.

FTIR spectral analysis. Ecorr, ba, and bc electrochemical parameters imply a mixed kind of inhibition. The SEM pictures clearly highlight the extract's protective properties on carbon steel via the creation of a passive layer. The foregoing findings clearly show that *Pisidium Guajava* extract may be used as a green corrosion inhibitor for carbon steel in HCl media.

M.Salasi et al. [89] They aimed to treatise the electrochemical behaviour of environment-friendly inhibitors of silicate and phosphonate in corrosion control of carbon steel in soft water media.

Using EIS and Tafel polarization methods, the inhibition efficiency of individual sodium silicate, HEDP, and their synergistic impact on the corrosion inhibition of carbon steel in aerated soft water solution were explored, and the following findings were obtained:

At 25 ppm concentration, HEDP demonstrated maximum corrosion inhibition of 62.59%, above which corrosion rate accelerates. This might be because HEDP acts as a rust remover at high quantities.

At 30 ppm concentration, sodium silicate inhibited corrosion by 54.76%, with greater quantities having a Detrimental impact. This behavior is connected to silicate self-polymerization at greater concentrations, as well as the silicate film properties that do not develop on their own.

The results of electrochemical impedance and Tafel polarization demonstrated that sodium silicate and HEDP work in tandem. At 15 ppm of sodium silicate and 10 ppm of HEDP, the highest value of S as a synergistic factor is 1.76 .

According to the findings, the inhibitor combinations had no influence on corrosion potential or Tafel slopes. As a result, it is inferred that mixed inhibition behavior predominates

SEM pictures and EDAX analysis demonstrated that HEDP was incorporated as phosphorous bonds via the silicate gel-like network, resulting in a synergistic action of the two inhibitors.

D. Sarada Kalyani et al. [90] The previous study was titled with electrochemical and surface analytical studies of carbon steel protected from corrosion in a law – chloride environment containing a phosphonate-based inhibitor. They found that corrosion inhibitor solution that is both effective and ecologically friendly. NTMP-Zn(II)-NA is a mixed type inhibitor that regulates both the anodic and cathodic partial reactions of carbon steel corrosion.

Also, In the presence of the ternary inhibitor formulation, the metal-solution interface undergoes considerable change, resulting in the creation of a protective surface coating. It takes 24 hours to create a protective coating on the majority of the metal surface. the film is smooth and consistent, with a minimal roughness.

The film is mostly composed of the polynuclear multiligand complexes Fe(III), Zn(II)-NTMP-NA, and $Zn(OH)_2$, with minor amounts of iron oxides and/or hydroxides.

A.Ruiz et al. [91] Revealed the soluble extract from *Opuntia Ficus-indica* (*Nopal* extract) as a green inhibitor due to its component called mucilage, which has the ability to retain water; for this reason, it has been used as metal corrosion protection in machinery pieces, tools and other metallic components that need to be stored for short periods. In this way, three industrial carbon steels (AISI 1018, 1045 and 4140) have been exposed in sulfuric acid (H_2SO_4) to evaluate the corrosion behavior with or without *Nopal* extract (NE). Some electrochemical techniques have been implemented to evaluate the corrosion inhibition efficiency (IE) such as DC linear polarization resistance (LPR) and AC electrochemical impedance spectroscopy (EIS). Results indicated a considerable superficial modification of steel in terms of dielectric constant and ion charge capacity. When the NE was added, the corrosion mechanism changed from localized to general attack, decreasing the corrosion rate in all cases. More susceptibility to fail by corrosion was observed in the 1045 carbon steel in comparison with the other two studied steels; these results were confirmed by the percentage of inhibitor's efficiency of about 95%.

It has been found that the inhibition performance and mechanism of *Loquat* leaves extract (LLE) for the corrosion of mild steel in 0.5 M H_2SO_4 were investigated using weight loss method, Electrochemical measurements and scanning electron microscope (SEM). The results revealed that LLE acted as a modest cathodic inhibitor, its inhibition

efficiency increased with the concentration of LLE and reached a maximum value of 96% at the 100% V/V concentration, but decreased with incremental temperature. Besides, it was found that the adsorption of LLE on steel surface obeyed Langmuir adsorption isotherm, and then the thermodynamic and kinetic parameters were further determined accordingly. Furthermore, LLE was preliminarily separated by pH-gradient sedimentation and the synergistic inhibition between the isolates was investigated [92].

The studies carried out many inhibitor additives during acidizing treatment in order to prevent excessive corrosion, prevent sludge and emulsions, prevent iron precipitation, improve cleanup, improve coverage of the zone, and prevent precipitation of reaction products. Foremost among acid additives are corrosion inhibitors; therefore compatibility of other additives with corrosion inhibitor is very critical to the success of acidizing treatment. Any additive that alters the tendency of the corrosion inhibitor to adsorb on casing and tubing will also change its effectiveness. In present work, the inhibitive action of henna extract on corrosion of N80 API steel in regular mud acid (HCl/HF 12/3 wt%) at 28 °C was investigated through electrochemical technique. After determining the optimum concentration of henna extract, effect of acid additives on inhibitive action of henna extract on corrosion behavior of N80 steel in regular mud acid was investigated through polarization measurement and electrochemical impedance spectrometry methods.

Inhibition efficiency of *Henna* extract as a corrosion inhibitor for N80 API steel in regular mud acid at 28 °C is 85.98% (average of three methods). The results show that except iron control additive, all additives decrease the performance of henna extract as corrosion inhibitor [93].

H.Bentrah et al. [94] Investigated the influence of temperature (25-65°C) on the adsorption and the inhibition efficiency of Gum Arabic (GA) for the corrosion of API 5L X42 pipeline steel in 1M HCl. The Inhibition behavior on steel in HCl has been studied in relation to the concentration of the inhibitor and the temperature using potentiodynamic polarization curves and electrochemical impedance spectroscopy.

Thermodynamic parameters of adsorption were calculated from the viewpoint of adsorption theory. The results show that at a temperature range from 25 to 65°C, GA was a good inhibitor for API 5L X42 pipeline steel, and its inhibition efficiency was significantly stable. the maximum inhibition efficiency (93%) is obtained at 4 $g.L^{-1}$. In absence and presence of GA, there is almost no change in the corrosion mechanism regardless of the temperature. The adsorption of GA on steel surface is an exothermic process. The

adsorption of GA involves physical adsorption. The use of GA as an eco-friendly corrosion inhibitor is practical for carbon steel in HCl.

The stability of inhibition efficiency of GA at a temperature range from 25 to 65°C could find possible applications in acid pickling, industrial acid cleaning and acid descaling.

1.3.2. Synergistic effect of green inhibitor with halide ions

The inhibitory effectiveness of corrosion inhibitors can be improved in a manner synergistic by the addition of halide ions in the corrosive environment. The synergy can be considered an effective method for reducing the quantity of inhibitors used and for diversify the application of inhibitor in a corrosive environment. It plays an important role only in theoretical research on corrosion inhibitors, but also in practical work. [95]

M. Djellab et al. [96] Identified the synergistic effect of halide ions and Gum Arabic for the corrosion inhibition of API5L X70 pipeline steel in H_2SO_4. They concluded that there was no synergistic impact between GA and the halides. The iodide ion had the strongest synergistic impact between GA and halide ions, with chloride and bromide ions coming in second with almost the same degree and the addition of iodide ions considerably improves the inhibitory efficacy of GA, increasing it from 52% to 99%.

The adsorption of GA alone and in conjunction with iodide ions on the surface of API5L X70 pipeline steel in sulfuric acid follows the Langmuir adsorption isotherm And potentiodynamic polarization results show that GA in combination with KI functions as a mixed-type inhibitor in sulfuric acid.

According to the standard adsorption free energy ($\Delta G°_{ads}$), GA adsorption comprises physical adsorption .While the trend of ($\Delta G°_{ads}$) which is more negative for the GA coupled with KI suggests physical and chemical adsorption.

The EIS results show that in the presence of large doses of KI (from 0.5 mM), the inductive loop vanishes and the Nyquist plots for GA-KI systems have only one depressed semicircle, corresponding to one capacitive loop.

A. Ridhwan, et al. [97] Studied the inhibitive effect of *Mangrove Tannin* (MT) on mild steel (MS) corrosion in 0.5 M hydrochloric acid solution was studied using electrochemical techniques and gravimetric method. The influence of halides KCl, KBr and KI on the corrosion inhibition of MT were also investigated. Results show that MT alone provided satisfactory inhibition on the corrosion of MS and it was also found that the

inhibition efficiency increased synergistically in the presence of halide ions. The synergistic effect of halide ions was found to follow the order: KI>KBr>KCl. The inhibitor reduced the corrosion rate through adsorption process and obeyed the Langmuir's adsorption isotherm.

R.Naderi et al. [98] Wanted to make an investigation on the inhibition synergism of new generations of phosphate-based anticorrosion pigments. They found that the corrosion inhibition synergism of zinc aluminum molybdenum orthophosphate hydrate (ZAM) and zinc calcium strontium aluminum orthophosphate silicate hydrate (ZCP) as new generations of phosphate-based anticorrosion pigments on mild steel dipped in 3.5% NaCl was investigated electrochemically and the following experimental evidences were obtained:

The trend and amplitude of low frequency impedance and noise resistance suggested that the modified pigments outperformed the traditional zinc phosphate, which was corroborated by corrosion current densities retrieved from polarization curves.

Lower electrochemical activity at the electrode/electrolyte interface in the presence of ZAM and ZCP was linked to the protective coating on the surface identified by SEM, as evidenced by a considerable drop in electrochemical current noise level and the appearance of the PSD plots. Furthermore, insignificant values of the characteristic charge as a parameter derived using shot noise theory revealed that in the case of new generations of phosphate-based anticorrosion pigments, the mass of metal lost in the corrosion event may be limited.

There was a strong trend connection between EN data and the findings of EIS and polarization studies.

Electrochemical noise tests confirmed the corrosion inhibition synergism provided by the combination of ZAM and ZCP, as did EIS and polarization. SEM surface investigation revealed a denser coating uniformly deposited on the surface in this example.

The EDX analysis results confirmed the electrochemical experiments indicating the combination of the two modified pigments is more efficient than each one alone in inhibiting mild steel corrosion.

Using XPS surface analysis, the precipitated layer in the instance of the combination of ZAM and ZCP was determined to be mostly constituted of zinc hydroxide/phosphate.

Furthermore, the role of several metal phosphates/oxides in the protective mechanism was validated.

S.Srinivasa Rao et al. [99] Wanted to study lactobionic acid as a New Synergist in Combination with Phosphonate-Zn(II) System for Corrosion Inhibition of Carbon Steel . They concluded that Lactobionic acid, a non-toxic organic molecule, has been shown to be a good synergist with PBTC and Zn^{2+} for corrosion control of carbon steel in a nearly neutral aqueous environment. Also ternary formulation comprising 20 mg L^{-1} PBTC, Zn^{2+}, and 30 mg.L^{-1} lactobionate is an excellent carbon steel corrosion inhibitor. Once the protective layer has established,the maintenance dosage will be a combination of 10 mg.L^{-1} PBTC, Zn^{2+}, and 20 mg.L^{-1} lactobionate. As a result, the ternary inhibitor system is more ecologically friendly. In addition to the inhibitor system works in the pH range of 5-8 and the inhibitor formulation functions as a mixed type inhibitor, suppressing both the anodic and cathodic reactions.

A significant change of the metal/solution interface occurs in the presence of the inhibitor formulation due to the creation of a thick protective coating besid the creation of a protective coating on the metal surface necessitates a 24 hour soaking period. Even at a higher temperature of 60 °C, the inhibitor formulation provides good inhibitory efficiency.

I.4.Phoenix dactylifera L

The fruit of date palm (Phoenix dactylifera L) is an important source of bioactive compounds [100]. There are more than 5000 date palm cultivars distributed around the world differing in nutritional, morphological, and genetic attributes, although commercial cultivars are limited in number [101]. Phoenix dactylifera is considered the most socioeconomically important tree because it has multipurpose uses including the utilization of dates as raw materials for an increasing number of food products [102].

They are an excellent source of simple carbohydrates mainly in the form of glucose and fructose (Table I.2); however, quantities of these components vary among cultivars and depend on the maturity stage [103, 108]. The partially ripen stage (Rutab) of the fruit has less total sugar than the fully ripened stage (Tamer).

In addition, dates are rich in dietary non-starch polysaccharides (NSPs) and some minerals such as potassium and magnesium [109, 111]. Bioactive constituents that have been detected in phoenix dactylifera fruits include phenolic acids, carotenoids, and flavonoids [112, 115].

I.4.1. Composition of Date

Throughout this section, we will use the word “date” to refer to the fleshy part of the fruit. Date, which is very sweet, comprises about 50–88% of the total weight according to cultivar, stage of ripening, and water content. Sugars make up about two thirds of date flesh with water about one fifth. the rest of date weight includes protein, fat, crude fiber, minerals, different vitamins (especially vitamin B), tannins, and many other components [116].

The main components of date and their quantities are given in Table I.2. Date has much nutritive value and can play an effective role in providing the nutritional needs of humans.

Each kilogram of fresh date contains approximately 1570 calories of energy, whereas dry date contains more than 3000 calories per kg [117].

Table I. 2:Main components of date

Constituents	Quantity (%)
Water	5–20
Sugar	44–88
Protein	1–7
Fat	0.1–0.5
Pectin	1–4
Ash	1–2.5
Crude fiber	3–18
Polyphenol	3

CHAPTER II

EXPERIMENTAL METHODS AND MATERIALS

This chapter describes the experimental, electrochemical and surface analysis methods used in this work. a description of the material, the electrolyte, the inhibitors studied and the assemblies carried out makes it possible, initially, to set an experimental approach ensuring good reproducibility of the results. The electrochemical techniques are in turn presented, so as to underline their interest in the study of inhibitors. The surface analysis method used makes it possible to provide information that is often complementary to the results obtained from electrochemical techniques.

II.1 Study techniques

To study corrosion phenomena in different corrosive environments and the properties of the inhibitor/halogen system, two types of methods have been adopted:

- The electrochemical methods allow first of all to have a better knowledge of the mechanism of corrosion in different corrosive environments, and to evaluate the effectiveness and the mechanism of action of the inhibitor / halogen system studied.
- Surface analyzes were used to determine the state of the working electrode and the nature of the layer that forms on its surface. thus, confirming the efficacy of the studied inhibitor/halogen system.

II.1.1. Electrochemical methods

The electrochemical methods used to study the corrosion phenomenon can be divided into two categories:

- Stationary electrochemical methods (example: polarization curves),
- Transient electrochemical methods. (example: electrochemical impedance spectroscopy).

II.1.1.1. Polarization curves

An electrochemical reaction on an electrode is governed by the overvoltage q applied, which is the difference between the electrode/solution potential E and the equilibrium potential of the reaction E_{eq} . The intensity of the current through this material is a function of the potential E, represented by a curve **i** = f (E), or log **i** = f (E), which is the sum of the currents of the electrochemical reactions occurring at the surface of the electrode. Its determination in a corrosive environment allows, among other things, the study of corrosion phenomena. Polarization curves are determined by applying a potential

between a working electrode and a reference electrode. A stationary current is established after a certain time (a few minutes to a few hours). It is measured between the working electrode and a counter electrode (or auxiliary electrode). From a kinetic point of view, two control modes are distinguished according to the limiting reaction step [118].

- Charge transfer at the metal/electrolyte interface (activation).
- Mass transport of electroactive species or reaction products.

The polarization curves of activation-controlled reactions follow a *Butler-Volmer law* [119].

$$1 = i.exp\left(\frac{\eta}{b_a}\right) - i.expi\left(\frac{\eta}{b_c}\right) \qquad \textit{Equation II. 1}$$

where i is the current density; i_0 , the exchange current density η, The overvoltage at the electrode (E - E_{corr}). Their plot on a logarithmic scale reveals, far from equilibrium, the existence of two linear branches, called Tafel lines, which signify that the reaction linked to the applied polarization is predominant. The slopes of the straight lines, or Tafel coefficients b_a and b_c and the exchange current density i_0 , linked to the rates of the partial anodic and cathodic reactions at equilibrium, are representative of the reaction mechanism and the rate of dissolution of the metal.

The polarization curves of the reactions controlled by diffusion satisfy Tafel's law for weak overvoltages but present a saturation of the current for strong overvoltages for which the diffusion of a species becomes limiting. The diffusion flux of this species at the electrode/solution interface then sets the reaction rate and therefore the intensity of the current [120].

II.1.1.2.Electrochemical impedance spectroscopy (EIS)

Electrochemical impedance spectroscopy (EIS) is widely used for studying the corrosion of uncoated materials or for measuring the protective power of organic coatings. For uncoated metals several works are devoted to this subject, we can summarize them simply by the fact that [121]:

- The impedance spectrum leads to the construction of an equivalent electrical circuit (CE).
- Among the constituent elements of the CE, we distinguish the non-Faradic

components and the double-layer capacity.

- The high frequency limit of the Faradaic impedance is associated with the charge transfer resistance, R_t . This resistance is most closely correlated with the rate of corrosion.
- At low frequencies, the contribution of the faradic process appears in the form of capacitive, inductive or elements with a frequency distribution (diffusion impedance for example)

Electrochemical impedance spectroscopy, as a function of frequency, can be represented either in the *Bode* , in the form of two curves:

- Log of the Z-log modulus of the frequency.
- Phase-log of the frequency.

Either in the form parametrized in frequency, in the complex plan known as of *Nyquist* :

- Real-opposite part of the imaginary part.
- In the *Nyquist plots* , each simple circuit element (resistor-capacitor or resistor-self-inductor in parallel) generates a semicircular locus, or impedance diagram, as seen in figure II.1[122] .

The Nyquist diagram obtained comprises one (or more) semi-circle(s) whose deviation at the origin indicates the resistance of the electrolyte R_S and the amplitude indicates the charge transfer resistance R_t .

Z_{Re} and Z_{Im} are the real and imaginary part of the impedance Z measured experimentally.

$$Z = Z_{re} + Z_{im} \qquad \textit{Equation II. 2}$$

The impedance measurement offers the possibility of ridding the raw values of R_P of their parasitic component R_S . this correction of the ohmic term is of primary importance in less conductive media.

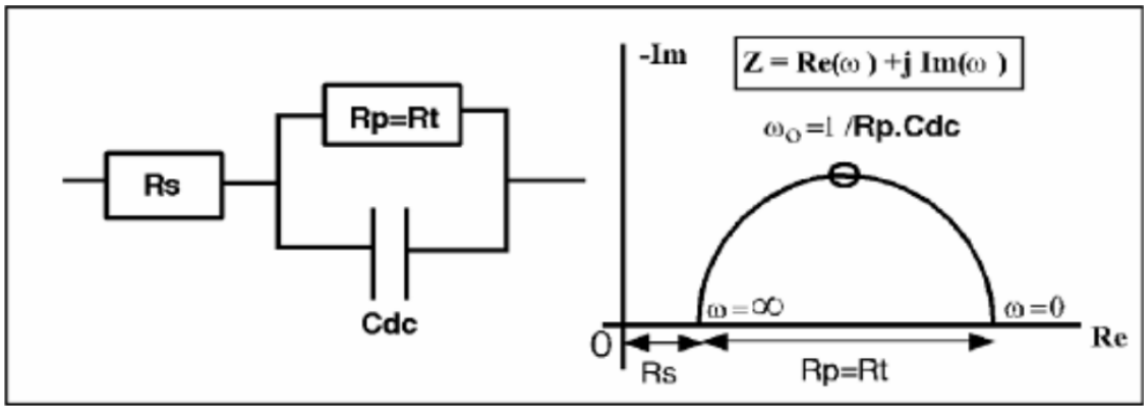

Figure II. 1: Circuit comprising the resistance of the solution Rs , in series with the assembly (Polarization resistance Rp , here confused with the charge transfer resistance Rt, in parallel with the double layer capacitor Cdl) . representation in the Nyquist plane of variations in its impedance

II.1.1.3.Impedance, polarization resistance and charge transfer resistance

Two cases can be distinguished:

The kinetics of corrosion is entirely fixed by the charge transfer reactions, in this case, the calculation of the so-called faradaic part of the impedance is reduced to deriving the intensity-potential relationship at the point considered. It is identified at any frequency with the bias resistance R_P, which then results from the charge transfer alone, represented in the general case by a resistance R_t, this case is illustrated in figure II.1 we therefore have $R_P = R_t$.

Other factors, such as mass transport, inhibition, surface film formation, surface partitioning between various electrochemical processes. It is established that the faradic impedance then comprises two types of components of radically different natures.

II.1.1.4. Critical analysis of measurement methods

Determining the corrosion current by plotting polarization curves or measuring impedance are currently the main means for comparing corrosion rates and potentials.

The results of the electrochemical measurements are used with Faraday's law to determine the kinetics of corrosion. This law relates the volume of corroded material to the corrosion current Icorr, but it can only be strictly applied in the case of uniform corrosion, in order to be able to correlate this rate of dissolution with a real degradation of the

material (reduction of thickness, for example). Localized corrosion in fact leads to faster degradation of materials than generalized corrosion, with an equivalent volume of dissolved matter.

These methods for evaluating the kinetics of corrosion do not then provide information on the morphology of the defects generated, likely to significantly modify the behavior of steel in the vicinity of its surface, nor on the level of localization of the corrosion.

II.2 EXPERIMENTAL

II.2.1.The working electrodes

II.2.1.1. Nomenclature

The designation of steel grades is a conventional means or system of naming, identifying, representing and even classifying them.

They are developed by entities or organizations involved in standardization, for example: european committee for standardization *(*CEN*),* International organization for standardization *(*ISO), or by professional organizations or certification associations, for example: *american iron and steel institute* (AISI) or *American petroleum institute* (API).

Carbon steel is a steel whose main alloying component is carbon, between 0.12 and 2.0%, the other alloying elements being in very small quantities.

American iron and steel institute *standard* defines that: steel is considered carbon steel when no minimum content is specified or required for, chromium (Cr), cobalt (Co), niobium (Nb), molybdenum (Mo), nickel (Ni), titanium (Ti), tungsten (W), vanadium (V) or zirconium (Zr) or any other element added to obtain the effect of desired alloy, when the maximum content prescribed for any of the following elements does not exceed the percentages indicated, i.e. 1.65% for manganese (Mn), 0.60% for silicon (Si), 0.60% for copper (Cu) [123]. It should be noted that the AISI, AFNOR, API, CEN, ISO standards are not the only ones to designate steels, in fact, according to each country, the nomenclatures differ.

The material used as the working electrode is a carbon steel used for the transport of hydrocarbons of API 5L X70 nomination, and meets the specification imposed by the API standard.

- The API (American Petroleum Institute) standard is designed to be acceptable to the petroleum industry according to the requirements of the legislation and the environment. API 5L X70 steel is designated by its elastic limit (70).
- API 5L means: pipeline.
- X70 means: the grade of steel. Other grades are, for example, A, B, X42, X60.
- The number 70 means: 70000 psi, it is the elastic limit of steel in psi (pound per square inch).

II.3 Material

The working electrode in this study was API 5L X70 pipeline steel. all samples destined for electrochemical experiments were cut into squares with the following dimensions 3 x 3 x 1 cm. The chemical composition of the studied steel was assured by the supplier, and contained in weight percentage: C 0.12 max, Mn 1.68 max, Si 0.27 min, P 0.012 max, S 0.005 max, Cr 0.051 max, Ni 0.04 max, Nb 0.033 max, Ti 0.03 max, and the balance Fe. The surface area of each working electrode that was exposed to the electrolyte was 2.85 cm^2. Before each test, the working surface was prepared by wet polishing with silicon carbide-abrasive papers with silicon carbide-abrasive papers (starting with grade 320 and ending with grade 800), rinsed with distilled water, and degreased with acetone.

II.4 Medium

Analytical reagent grade 96 % sulfuric acid and distilled water were used to prepare the electrolyte solutions (0.5 $mol.L^{-1}$).

II.5 Inhibitor

The Ghars Dates were collected from phoenix dactylifera (Date Palm) at Biskra (southeast Algeria), in September 2021. The Ghars date extract was secreted spontaneously and naturally (without any process) at air temperature. The extract of Ghars date was selected for the present study and used as a corrosion inhibitor.

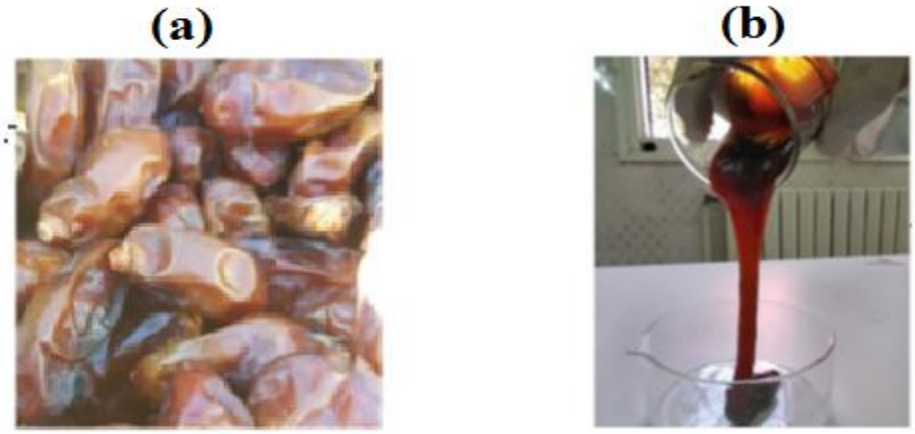

Figure II. 2: (a) ghars date (GD) (b) ghars date extract (GDE)

The principal constituent of polysaccharides in date fruits is galacturonic acid. [124] The molecular structure of galacturonic acid and some phenolic compounds (cyanidin, **[**1**25]** apigenin and gallic acid [126]) for date fruits was shown in Fig. II.3.

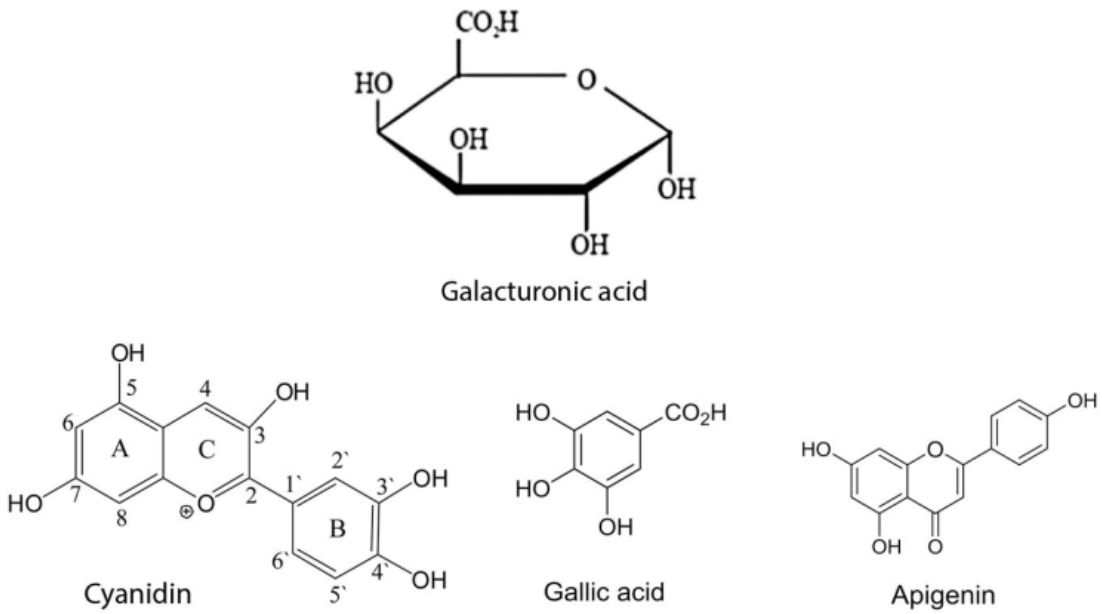

Figure II. 3: The molecular structure of galacturonic acid and some phenolic compounds.

II.6 .Electrochemical techniques

Electrochemical impedance spectroscopy (EIS) and potentiodynamic polarization (PDP) were adopted to study the inhibition effect of the GDE and GDE/iodide ions system

for API 5L X70 pipeline steel in 0.5 mol L^{-1} sulfuric acid at 20 °C. All tests were carried out in an electrochemical cell (para cell electrochemical cell kit) that was designed to hold a working (API 5L X70 pipeline steel), reference (Ag/AgCl), and counter electrode (graphite). the working electrode and either a graphite counter electrode were placed in an opposed geometry.The electrochemical cell was connected to a Gamry instruments potentiostat/galvanostat/ZRA (reference 3000). The Gamry applications included software namely Gamry instruments framework (for the piloting of hardware) and Gamry Echem analyst software (for data processing). All electrochemical tests of the API 5L X70 steel were performed in 0.5 mol.L^{-1} sulfuric acid medium without (blank) and with inhibitor (GDE or GDE/iodide ions system) after 30 minutes of immersion at 20 °C. Tafel curves were achieved by changing the working electrode potential from -0.25 to +0.25 V versus open-circuit potential (OCP) at a scan rate of 0.5 mVs^{-1}. The anodic (ba) and cathodic (bc) Tafel slopes were extrapolated to determine the corrosion current (Icorr). The inhibition efficiency (η_{pol}) was calculated using Equation II.3

$$\boldsymbol{\eta_{pol}}\% = \frac{\boldsymbol{Icorr - Icorr(inh)}}{\boldsymbol{Icorr}} \times \mathbf{100} \qquad \textit{Equation II. 3}$$

where Icorr(inh) and Icorr represent corrosion current density with and without inhibitor, respectively.

EIS experiments were carried out under potentiostatic conditions over a frequency range from 20 kHz to 50 mHz, with an amplitude of 10 mV peak-to-peak. the Inhibition efficiency (η_{EIS}) was calculated by comparing the values of the charge transfer resistance in the presence (R_t) and absence ($\acute{R}_t$) of the GDE or GDE/iodide ions system as follows (Equation II.3):

$$\boldsymbol{\eta_{EIS}}\% = \frac{\boldsymbol{R_t - \acute{R}_t}}{\boldsymbol{R_t}} \times \mathbf{100} \qquad \textit{Equation II. 4}$$

II.7 Surface study by scanning electron microscopy (SEM-EDX)

Surface morphologies of the samples (API 5L X70 pipeline steel with dimensions of 1 × 1 × 1 cm) were exposed to 0.5 mol.L^{-1} sulfuric acid without and with inhibitor (GDE or GDE/iodide ions system) at 20 °C were analyzed. Scanning electron microscopy (SEM) images and energy-dispersive X-ray spectroscopic analysis (EDX) were acquired by TESCAN VEGA3 scanning electron microscope.

II.8 . Fourier transform infrared spectroscopy (FTIR)

Fourier Transform Infrared spectroscopy (FTIR) is a largely used technique to identify the functional groups in the materials (gas, liquid, and solid) by using the beam of infrared radiations. An infrared spectroscopy measured the absorption of IR radiation made by each bond in the molecule and as a result gives spectrum which is commonly designated as % transmittance versus wave number (cm^{-1}).

CHAPTER III

RESULTS AND DISCUSSION

In this part is devoted to the evaluation of the corrosion of API 5L X70 steel in a sulfuric acid environment. For this, a series of electrochemical tests and surface analyzes were carried out. From the electrochemical tests the corrosion rate, corrosion potential, charge transfer resistance and double layer capacitance were determined. Examination of the surface by scanning electron microscopy (SEM) and energy dispersive spectrometry (EDX) were used to determine the type of corrosion of API 5L X70 steel in H_2SO_4 medium and thus to determine the composition of corrosion products in a qualitative manner.

III.1.FTIR spectra of the GDE

Fig. III.1 illustrates the FTIR spectrum of the GDE sample. This figure shows the links with the following wave numbers: 3363, 2927, 2365, 1626, 1411and 1053 cm^{-1}.

A broadband at a range of 3604-3003 cm^{-1} concentrated at 3363 cm^{-1} was attributed to the O–H stretching vibration of intra- and inter-molecular hydrogen bonds. [127,128] An absorption band at 2927 cm^{-1} was attributed to the C–H stretching of the CH, CH_2, and CH_3 of the methyl groups in the sugar ring. [127] The peak recorded at 2365 cm^{-1} indicated the existence of aliphatic C–H bonds. The strong absorption detected at 1626 cm^{-1} indicated the presence of the C=O asymmetric stretching vibration of carboxylate (COO^-) groups.[128] Other important absorption peak detected at 1411 cm^{-1} was assigned the symmetric (COO^-) stretching mode, which indicates the presence of uronic acid, namely galacturonic acid, in the polysaccharides. The important peak at around 1553 cm^{-1} detected a pyranose form of sugars.[129] These results indicate that GDE contains various functional groups, namely the carboxyl group and hydroxyl group. Similar results were obtained in the work of Trigui et al. [130] and Ghribi et al. [131] For water-soluble polysaccharides of black cumin seeds and polysaccharides of chickpeas, respectively.

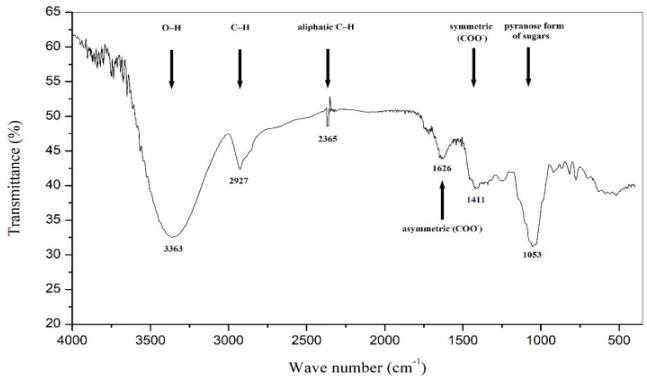

Figure III. 1.FTIR spectra of GDE.

III.2. Inhibition effect of the GDE in sulfuric acid

III.2.1.Impedance measurements

The study investigated the corrosion behaviour of API 5L X70 pipeline steel in 0.5 mol.L^{-1} sulfuric acid at 20 °C, both with and without different concentrations of the GDE, using electrochemical impedance spectroscopy. The EIS plots are shown in Fig. III.2, with (a) Nyquist, (b) Bode modulus, and (c) Bode phase angle. Table III.1 provides the electrochemical parameters that were exploited from the Nyquist plots. The plots displayed semi-circles with their centres under the real axis, which increased in size with inhibitor concentration, indicating a charge transfer process primarily controlling carbon steel's corrosion.[132] This behaviour is typical of solid electrodes, called frequency dispersion, due to dislocations, adsorption of inhibitors, surface roughness, fractal structures, distribution of activity centres, impurities, and formation of porous layers. [133] The EIS plots in Figure III.2a exhibit a similar shape, with a large capacitive loop at high frequencies and an inductive loop at low frequencies, both with and without an inhibitor. Two-time constants for iron dissolution at Ecorr have been reported in previous studies.[134] The large capacitive loop at high frequencies observed in Figure III.2a can be explained by the double-layer capacity running parallel to the charge transfer resistance (R_t). Meanwhile, the inductive loop at low frequencies may have resulted from the relaxation process arising from adsorbed species such as proton and sulfate ions on the metal surface. Additionally, it could have been caused by the re-dissolution of the passivated surface at low frequencies.[135] It can be observed from Fig. III.2b that the inhibition efficiency increases as the concentration of inhibitor increases, as evidenced by the increase in impedance plots at low frequencies in the Bode plots. This increase in inhibition efficiency is attributed to the adsorption of the GDE compounds on the surface of API 5L X70 pipeline steel in 0.5 mol.L^{-1} sulfuric acid. The same behaviour was reported by Haladu et al. [136]

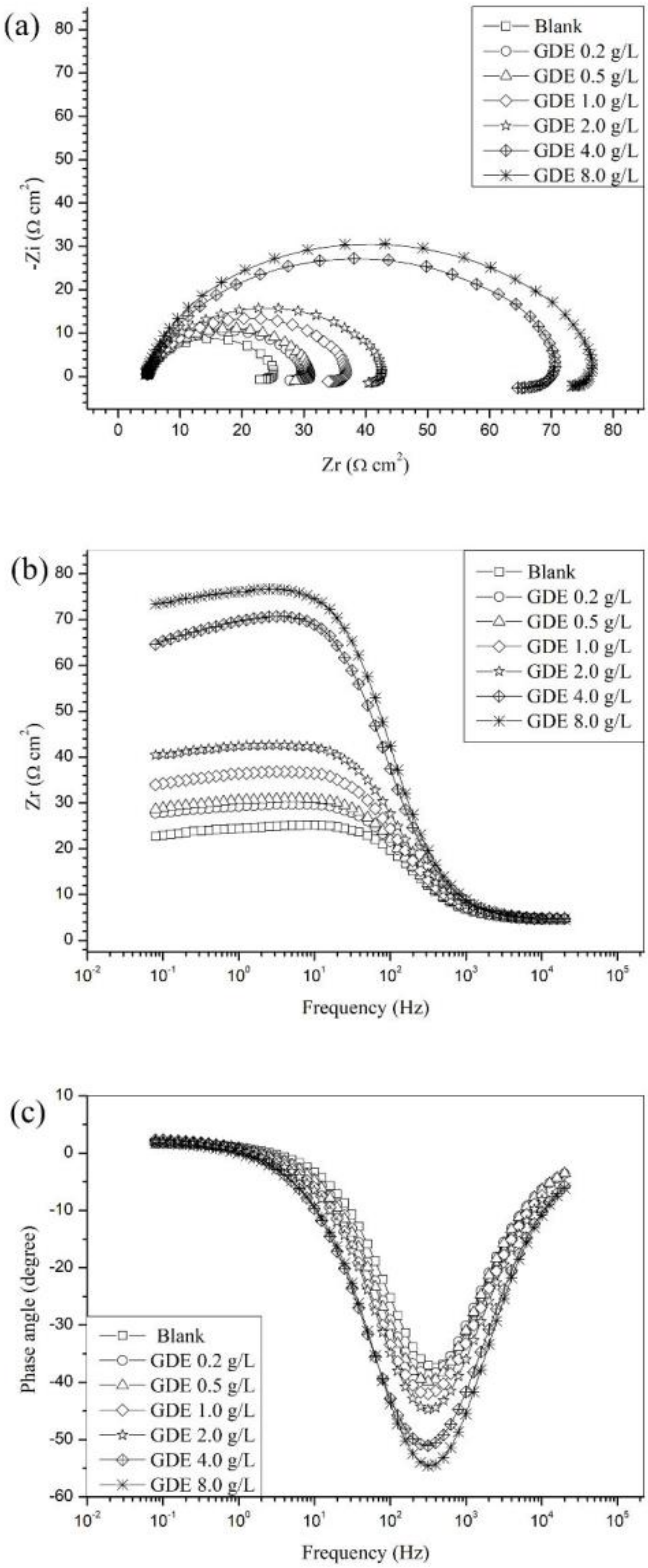

Figure III. 2. EIS plots for API 5L X70 pipeline steel in 0.5 mol.L^{-1} sulfuric acid without and with different concentrations of the GDE at 20 °C, (a) Nyquist, (b) Bode modulus, and (c) Bode phase angle representations.

Table III. 1. EIS parameters for API 5L X70 pipeline steel in 0.5 mol.L^{-1} sulfuric acid without and with different concentrations of the GDE at 20 °C

System/ concentration	Rs (Ω cm^2)	Y_0 (μΩ S cm^{-2})	n	Rt (Ω cm^2)	L (H cm^2)	RL (Ω cm^2)	C_{dl} (μF cm^{-2})	η_{EIS} (%)
Blank	4.8	120	0.88	20.7	40	300	294	-
0.20 g L^{-1}	4.6	150	0.88	25.0	60	380	233	17.2
0.50 g L^{-1}	4.6	102	0.88	26.3	50	380	222	21.2
1.00 g L^{-1}	4.8	100	0.88	32.2	50	362	217	35.7
2.00 g L^{-1}	4.9	98	0.88	38.0	45	300	213	45.5
4.00 g L^{-1}	4.6	65	0.89	66.0	50	480	125	68.6
8.00 gL^{-1}	4.6	62	0.88	72.0	60	600	123	71.2

As shown in Fig. III.2c, the phase angle plots suggest that there is a correlation between the concentration of the inhibitor and its inhibitive behaviour, which is attributed to the adsorption of more inhibitor molecules onto the metal surface at higher concentrations. In this study, impedance data was collected and analysed to model the steel/solution interface in the presence and absence of the inhibitor, using an electrical equivalent circuit diagram presented in Fig. III.3. The circuit model comprises several elements, including the solution resistance Rs, the charge transfer resistance Rt, inductive elements RL and L, and a constant phase element (CPE), which is essential to account for frequency dispersion commonly associated with surface heterogeneity.[137]

The experimental data were fitted to the electrical equivalent circuit model described in Fig. III.3, resulting in an excellent fit for all collected data.

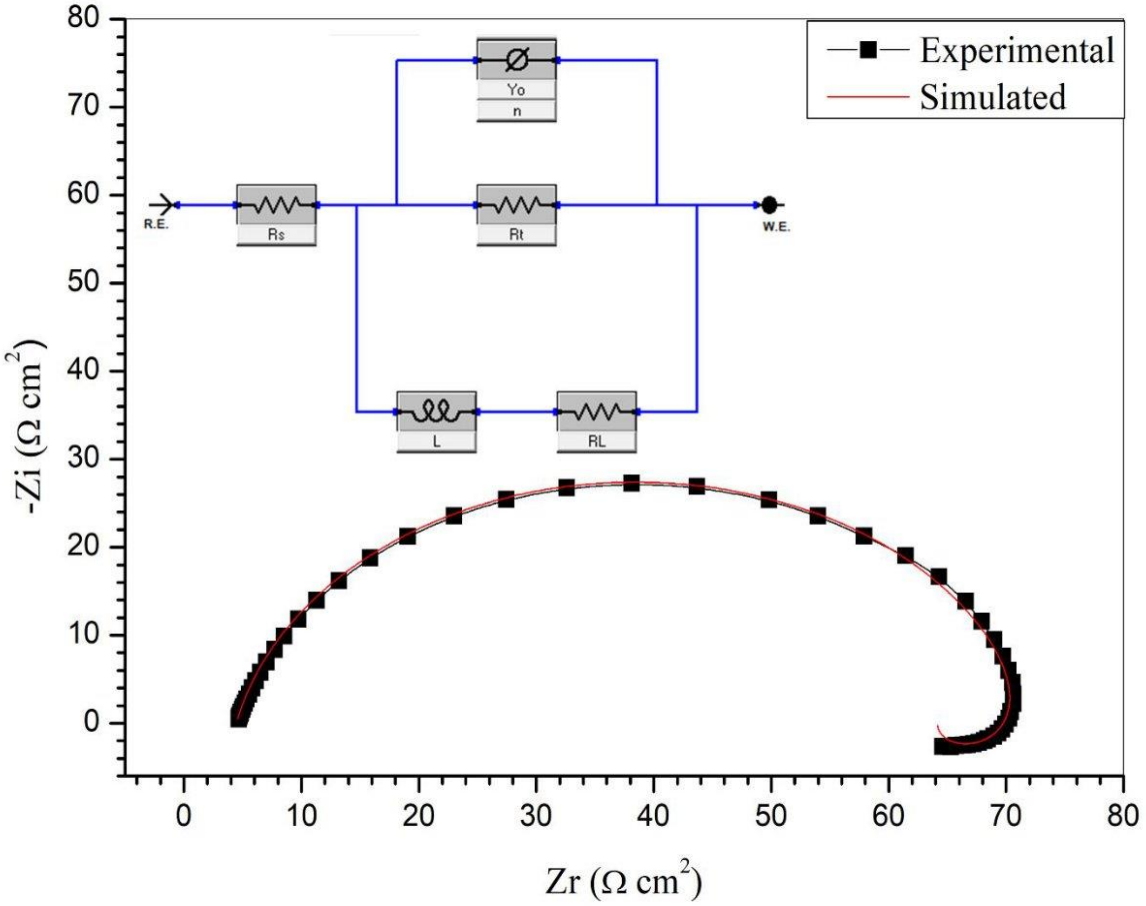

Figure III. 3.Nyquist plot of simulated data and experimental data, together with the equivalent circuit used to fit the impedance data, recorded for API5L X70 pipeline steel in 0.5M H_2SO_4 containing 4 g.L^{-1} GDE.

The impedance function of the CPE is described as follows (Equation III.1). [138]

$$Z_{CPE} = Y_0^{-1}(j\omega)^{-n} \qquad \textit{Equation III. 1}$$

where Y_0 represents the magnitude of the CPE, ω is the angular frequency, j is the imaginary root, and n is the deviation parameter. The double layer capacitance C_{dl} was determined using Equations 4, as described as follows[139].

$$C_{dl} = Y_0(2\pi f_{max})^{n-1} \qquad \textit{Equation III. 2}$$

The frequency at which the imaginary component of impedance reaches its maximum value is denoted as fmax.

As illustrated in Fig.III.2a, the Nyquist plots underwent significant changes upon the addition of the inhibitor. The impedance of the inhibited system increases in proportion to

the inhibitor concentration. The Rt value increased with an increase in the inhibitor concentration, indicating higher inhibiting power, as reported in Table III.1. Notably, the maximum inhibitive effect and highest charge transfer resistance were observed at a GDE concentration of 4 $g.L^{-1}$. A high charge transfer resistance reflects a slower corroding system. On the contrary, the C_{dl} values tended to decrease with an increase in the concentration of the GDE compounds, which led to an increase in inhibition efficiency, as also reported in Table 1. The decrease in C_{dl} values can be attributed to a decrease in the local dielectric constant and/or to an increase in the thickness of the electrical double layer. This suggests that the GDE molecules act by adsorption at the metal/solution interface[140].

It is evident from the results presented in Table III.1 that the corrosion of API 5L X70 pipeline steel in 0.5 mol L^{-1} sulfuric acid is governed by the charge transfer mechanism and that the inhibition of corrosion is facilitated through the adsorption of the GDE compounds onto the surface of the steel. As shown in Table III.1, for 4 $g.L^{-1}$ of the GDE, the inhibition efficiency was at a maximum (68.6 %) and did not change with great value.

III.2.2.Potentiodynamic polarization measurements

Fig. III.4 displays the potentiodynamic polarization curves for API 5L X70 pipeline steel in 0.5 $mol.L^{-1}$ sulfuric acid at 20 °C with different concentrations of the GDE. The purpose of the potentiodynamic polarization experiments was to determine the impact of the GDE on the anodic dissolution of API 5L X70 pipeline steel and cathodic hydrogen ion reduction. The values of Icorr, Ecorr, and Tafel slopes (bc and ba) were calculated by extrapolating the linear Tafel segments of the cathodic and anodic curves (Table III.2).

Table III.2 shows the data, including η%, which indicates that the addition of the GDE to the acid solution results in a significant decrease in the Icorr value while the Ecorr value shifts slightly towards a more negative direction at a given temperature.

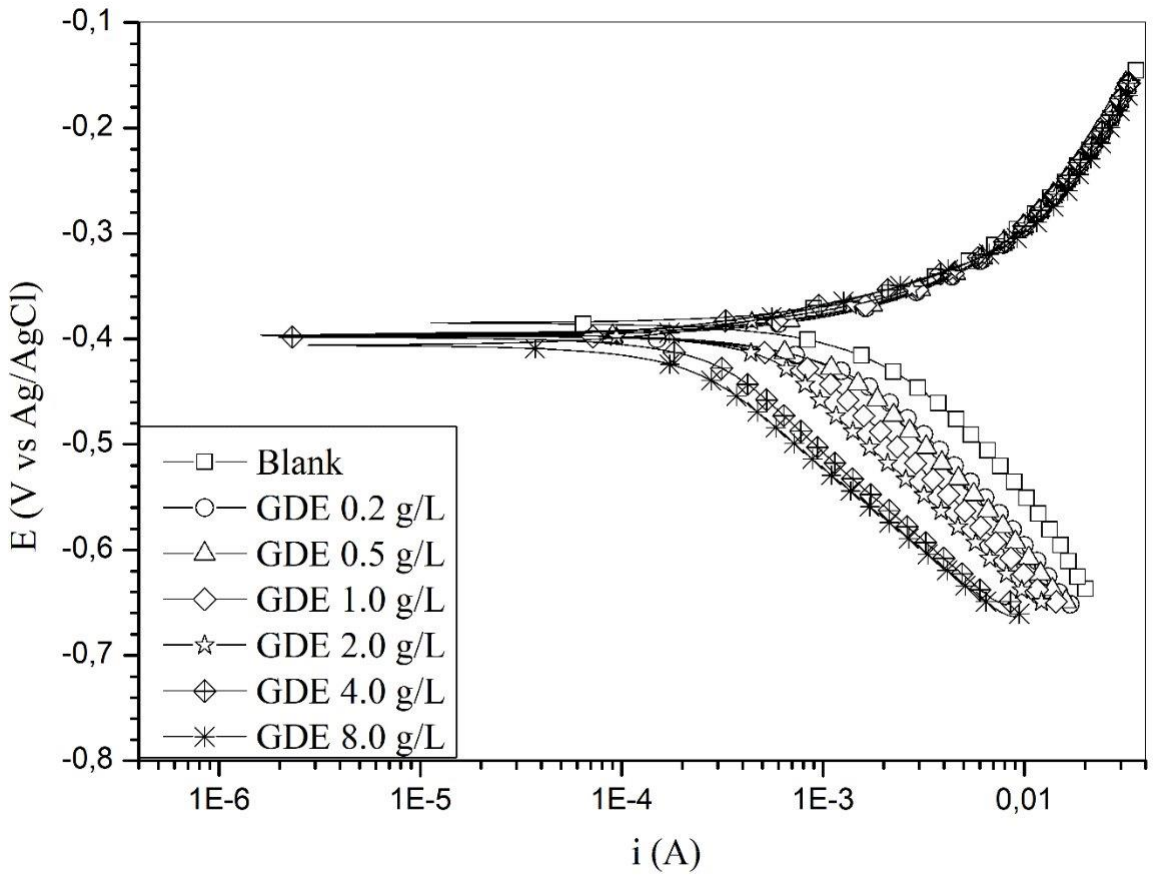

Figure III. 4.Potentiodynamic polarization curves for API5L X70 pipeline steel in 0.5M H_2SO_4 without and with different concentrations of GDE at 20 °C.

The greatest shift in Ecorr value, which is observed at a concentration of 8 $g.L^{-1}$, is 20 mV, which is much lower than 85 mV. Therefore, the magnitude of the shift is not large enough to determine whether the inhibitor is cathodic or anodic.[141] However, ba and bc values remain slightly changed, implying that the inhibitor reduces the anodic and cathodic process rate possibly through adsorption. In this case, it is difficult to determine whether the cathodic or anodic reaction is predominantly inhibited, and therefore, it is appropriate to classify the inhibitor as a mixed inhibitor. The results indicate that the inhibition efficiency rises as the inhibitor concentration increases, with the highest efficiency of 74 % achieved at a concentration of 4 $g.L^{-1}$ of GDE. These findings are in good accordance with those obtained through electrochemical impedance spectroscopy.

Table III. 2. Potentiodynamic polarization parameters for API 5L X70 pipeline steel in 0.5 mol.L^{-1} H_2SO_4 without and with different concentrations of the GDE at 20 °C.

Concentration	Ecorr (mV)	I_{corr} ($\mu A\ cm^{-2}$)	- bc ($mV\ dec^{-1}$)	ba ($mV\ dec^{-1}$)	η_{pol} (%)
Blank	-386	1540	189	87	-
0.20 g L^{-1}	-397	1160	209	80	24
0.50 g L^{-1}	-395	1080	228	73	30
1.00 g L^{-1}	-396	847	280	63	45
2.00 g L^{-1}	-395	681	281	65	55
4.00 g L^{-1}	-398	391	282	68	74
8.00 g L^{-1}	-406	721	254	92	75

III.2.3. Adsorption isotherm and standard adsorption free energy of the GDE

Various adsorption isotherms were evaluated in the current investigation, and it was discovered that the Langmuir adsorption isotherm provided the most accurate explanation for the adsorption behaviour of the inhibitor under investigation . The Langmuir adsorption isotherm can be used to establish a correlation between the surface coverage ($\theta = \eta_{EIS}$ %/100) and the inhibitor concentration (C) in the electrolyte (Equation III.3) [142].

$$\frac{C}{\theta} = \frac{1}{K_{ads}} + C \qquad \textit{Equation III.3}$$

The constant of adsorption is represented by K_{ads}. When plotting C/θ against C at 20 °C, a straight line is obtained with a slope value that is nearly equal to 1. By using the adsorption constant (K_{ads}), the standard free energy of adsorption ($\Delta G°_{ads}$) can be calculated via Equation III.4 : [143]

$$\Delta G^{o}{}_{ads} = -RT\ ln(1 \times 10^{6} K_{ads}) \qquad \textit{Equation III.4}$$

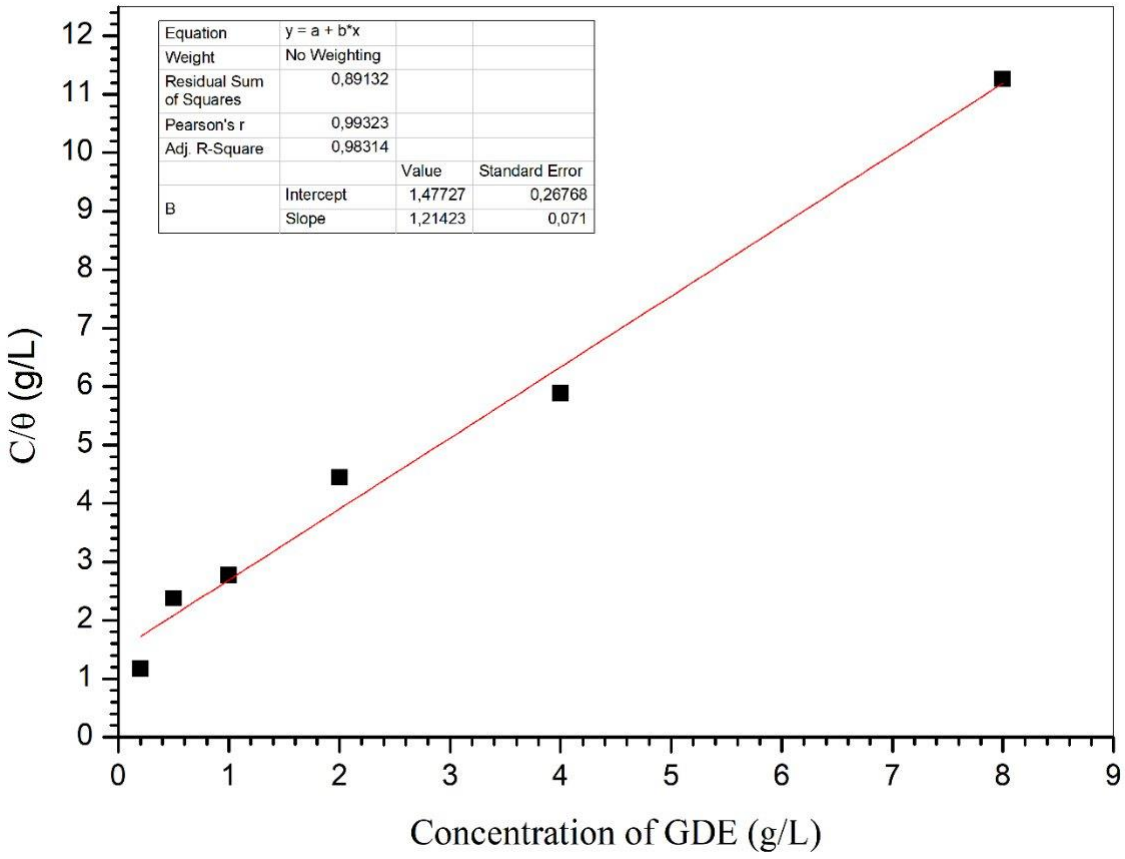

Figure III. 5.Langmuir isotherm adsorption mode of GDE on the API 5L X70 pipeline steel in 0.5 M H_2SO_4 *at 20 °C (from EIS measurements).*

Table III.3 lists the values for $\Delta G°_{ads}$ and K_{ads}, where K_{ads} can be considered as an indicator of the adsorption strength between inhibitor molecules and the metal surface.[144]The concentration of water molecules in $mg.L^{-1}$ is denoted by 1×10^6, and R represents the universal gas constant while T signifies the absolute temperature. typically, $\Delta G°_{ads}$ values ranging up to -20 kj mol^{-1} signify physical adsorption, which is characterized by electrostatic interaction between charged molecules and a charged metal. In contrast, values below -40 kJ mol^{-1}indicate chemisorption, where there is sharing or transfer of charge from the inhibitor components to the metal surface to form a coordinate bond[145]. As per the findings of this study, the value of $\Delta G°_{ads}$ is -16.12 kJ mol^{-1}, indicating that the GDE is adsorbed on the surface of API 5L X70 pipeline steel by physisorption.

Table III. 3.Langmuir adsorption isotherm parameters for API 5L X70 pipeline steel in 0.5 mol L^{-1} H_2SO_4 containing the GDE at 20 °C.

Isotherm mode	Linear correlation coefficient	Slope	K_{ads} ($L\ g^{-1}$)	$\Delta G°_{ads}$ ($kJ\ mol^{-1}$)
Langmuir	0.99323	1.21	0.67	-16.12

III.3.Synergistic effect of the GDE with iodide ions

III.3.1.Electrochemistry measurements

In a previous study, the inhibition efficiency of iodide ions in 0.5 $mol.L^{-1}$ sulfuric acid was studied. The inhibition efficiency was found maximum of up to 66 % for 5×10^{-4} $mol.L^{-1}$ of potassium iodide at 20 C°. In this study, the concentration of 5×10^{-4} $mol.L^{-1}$ of potassium iodide was adopted to study the synergistic effect of the GDE with iodide ions.

Fig. *III. 6* displays the polarization curves of API 5L X70 pipeline steel when it is placed in a 0.5 $mol.L^{-1}$ sulfuric acid with different concentrations of the GDE in the presence of 5×10^{-4} $mol.L^{-1}$ of potassium iodide. The electrochemical parameters derived from this experiment are presented in Table III.4. It can be observed from Figure 7 and Table III.4 that the addition of potassium iodide results in a significant decrease in the corrosion current density, and a shift in the corrosion potential towards a more positive direction. Furthermore, the inhibition efficiency greatly improves when the potassium iodide is added, suggesting that the adsorption protective layer on the electrode surface becomes completer and more stable in the presence of potassium iodide than with the GDE alone in the 0.5 $mol.L^{-1}$ sulfuric acid.

Based on the change in the Ecorr values of inhibited steel samples with respect to the Ecorr results of uninhibited steel specimens, investigated GDE/iodide ions system may be classed as anodic, cathodic, or mixed kinds of inhibitors. The GDE/iodide ions system had the greatest range in Ecorr values of 62 mV. A change in Ecorr values of less than 85 mV indicates that the GDE/iodide ions system acts as a mixed kind of corrosion inhibitor. Moreover, the GDE/iodide ions system reduces the rate of both anodic metallic dissolution and cathodic hydrogen evaluation procedures significantly.

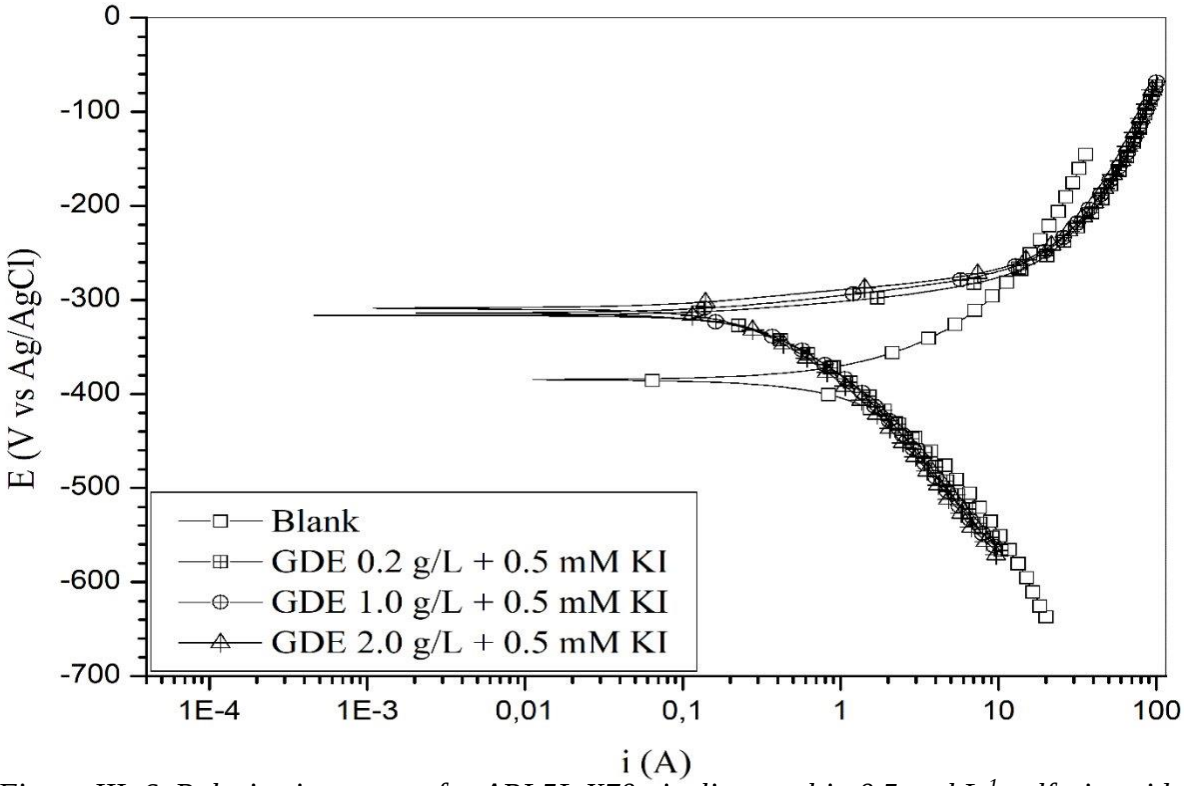

Figure III. 6. Polarization curves for API 5L X70 pipeline steel in 0.5 mol.L^{-1} sulfuric acid containing different concentrations of the GED combined with 5×10^{-4} mol.L^{-1} of potassium iodide (KI) at 25 °C.

Table III. 4. Potentiodynamic polarization parameters for API 5L X70 pipeline steel in 0.5 mol.L^{-1} H_2SO_4 containing different concentrations of the GDE combined with 5×10^{-4} mol.L^{-1} of potassium iodide (KI) at 25 °C.

Concentration	Ecorr (mV)	I_{corr} (μA cm^{-2})	- bc (mV dec^{-1})	ba (mV dec^{-1})	η_{pol} (%)
Blank	-386	1540	189	87	-
0.20 g L^{-1} GDE + 5×10^{-4} mol L^{-1} KI	-311	280	123	17	93.19
1.00 g L^{-1} GDE + 5×10^{-4} mol L^{-1} KI	-306	252	123	18	93.80
2.00 g L^{-1} GDE + 5×10^{-4} mol L^{-1} KI	-300	232	140	15	94.36

For testing the synergistic effect of the GDE/iodide ions system on the corrosion inhibition of API 5L X70 pipeline steel in 0.5 mol.L^{-1} sulfuric acid at 25 °C, EIS measurements were performed using a fixed concentration of potassium iodide (5×10^{-4} mol L^{-1}) paired with varying concentrations of the GDE (0.2, 1.0, and 2.0 g.L^{-1}). The Nyquist plots of pipeline steel in 0.5 mol.L^{-1} sulfuric acid at 25 °C using a GDE/iodide ions system are shown in Fig. III.6.

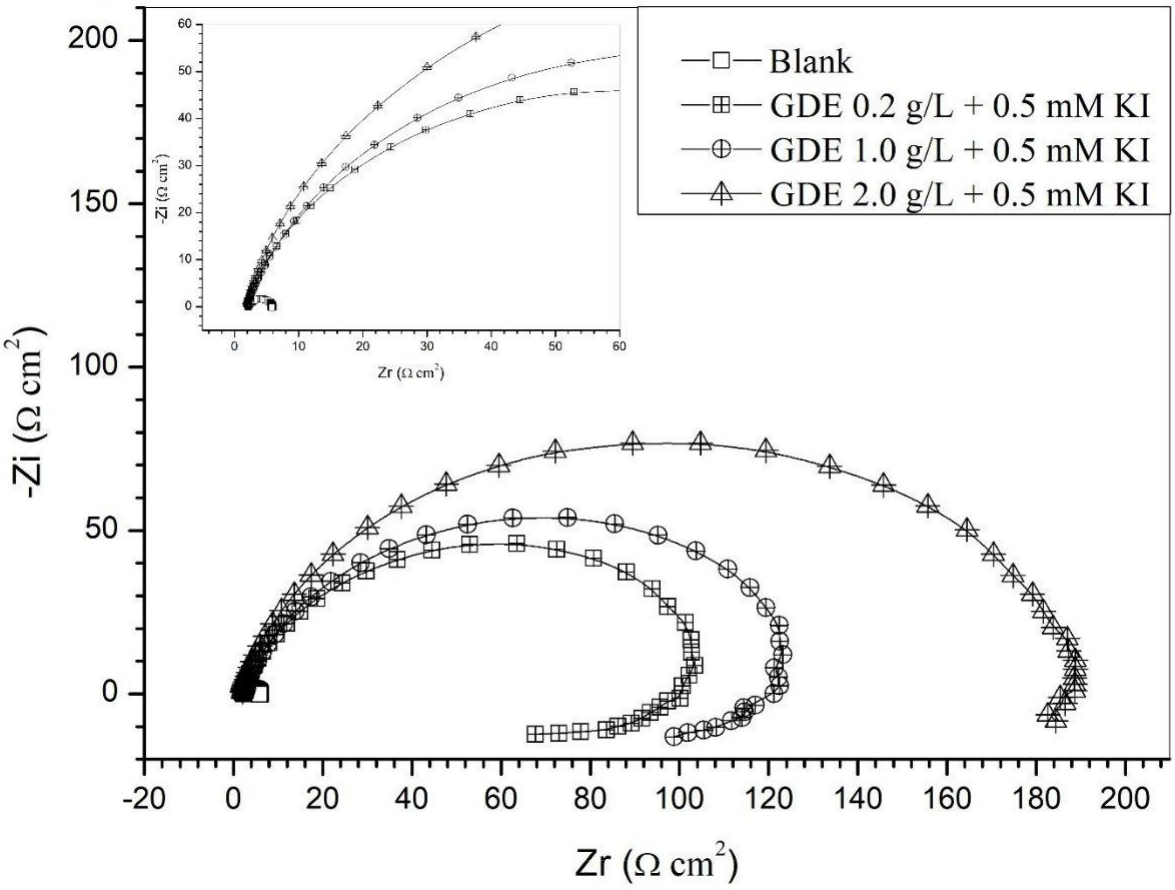

Figure III. 7. Nyquist plots for API5L X70 pipeline steel in 0.5 mol.L^{-1} sulfuric acid without and with different concentrations of the GDE combined with 5×10^{-4} mol.L^{-1} of potassium iodide (KI) at 25 °C.

Fig. *III. 8.* indicates that the diameters of the semicircles increased in size with the GDE concentrations that were added to 0.5 mol L^{-1} sulfuric acid containing 5×10^{-4} mol.L^{-1} of potassium iodide. The results clearly reveal that the GDE/iodide ions system has a significant synergistic effect on the corrosion behaviour of pipeline steel. It can be observed that the complex plane impedance exhibits one capacitive loop at high frequencies and one inductive loop at low-frequency values indicating the presence of two-

time constants when the GDE/iodide ions system is present. The equivalent circuit depicted in Fig. 4 was used to fit the experimental data acquired from the impedance measurements, and the electrochemical parameters obtained were listed in Table III.5.

Table III. 5. EIS parameters for API 5L X70 pipeline steel in 0.5 mol.L^{-1} sulfuric acid containing different concentrations of the GDE combined with 5×10^{-4} mol.L^{-1} of potassium iodide (KI) at 25 °C.

System/ concentration	Y_0 ($\mu\Omega$ S cm^{-2})	n	Rt (Ω cm^2)	L (H cm^2)	RL (Ω cm^2)	C_{dl} (μF cm^{-2})	η_{EIS} %
Blank	275	0.88	3.9	19.5	130	220	-
0.20 g L^{-1} GDE	150	0.88	25.0	60	380	233	17.0
0.20 g L^{-1} GDE + 5×10^{-4} mol L^{-1} KI	222	088	101.0	20	268	62	96.1
1.00 g L^{-1} GDE	100	0.88	32.2	50	362	217	35.7
1.00 g L^{-1} GDE + 5×10^{-4} mol L^{-1} KI	130	088	122.0	70	600	33	96.7
2.00 g L^{-1} GDE	98	0.88	38.0	45	300	213	45.5
2.00 g L^{-1} GDE + 5×10^{-4} mol L^{-1} KI	123	0.87	191.9	1200	2000	32	97.9

According to the data presented in Table III.5, the addition of 5×10^{-4} mol.L^{-1} of potassium iodide with various concentrations of the GDE (0.2, 1.0, and 2.0 g.L^{-1}) resulted in a rise in charge transfer resistance (Rt), reaching a maximum value of 191.9 Ω cm^2 for 2 g.L^{-1}GDE + 5×10^{-4} mol.L^{-1} of potassium iodide.By contrast, in the presence of only 2 g.L^{-1} GDE, the Rt value was only 45.5 Ω cm^2. The results indicated that the presence of the GDE/iodide ions system (2 g.L^{-1} GDE + 5×10^{-4} mol.L^{-1} of potassium iodide) caused a decrease in double-layer capacitance (C_{dl}) from 213 µF cm^{-2} (observed in the presence of 2 g.L^{-1} GDE alone) to 32 µF cm^{-2}. Furthermore, the inhibition efficiency values reached 97.9 %, which is a significant increase. It is worth noting that the data obtained from polarization curves and impedance spectra showed similar trends and were in good agreement.

The degree of synergism between the GDE and potassium iodide was evaluated by calculation of the synergism parameter S which was provided by Hackermann and Aramaki (Equation).

$$S = \frac{1-\eta_1-\eta_2+(\eta_1\times\eta_2)}{1-\eta_{12}} \qquad \textit{Equation III. 5}$$

Where η_1 and η_2 are the inhibition efficiencies of the GDE and potassium iodide, when they act alone in 0.5 mol.L^{-1} sulfuric acid, and η_{12} is the inhibition efficiency for the simultaneous addition of the GDE and of potassium iodide at the same concentrations the concentrations of the GDE and potassium iodide when they act alone). The value of S>1 indicates a synergistic effect between the potassium iodide and the studded inhibitor (GDE), and cooperative adsorption occurs, while if S <1, antagonistic comportment dominates and competitive adsorption takes place. In cooperative adsorption, one substance (GDE or potassium iodide) is chemisorbed on the steel surface while the other is physisorbed. In competitive adsorption, the GDE and potassium iodide can be adsorbed simultaneously but at diverse-active sites on API 5L X70 steel surface.

Depending on the inhibition efficiency equals 66% for steel in 0.5 mol.L^{-1} sulfuric acid containing 5×10^{-4} mol.L^{-1} of potassium iodide, the synergism parameter S was 7.23, 6.62 and 8.82 for the concentrations 0.2, 1.0 and 2.0 g.L^{-1} GDE respectively, which indicates that there is a true synergism between the potassium iodide and GDE in 0.5 mol L^{-1} sulfuric acid with cooperative adsorption.

III.3.2.Adsorption isotherm and standard adsorption free energy of GDE/iodide ions system

Temkin, Langmuir and Frumkin adsorption isotherms were evaluated for the GDE/iodide ions system in 0.5 mol.L^{-1} sulfuric acid for API 5L x70 pipeline steel. The best fitting for EIS data, with a slope very close to 1, is corresponded to Langmuir isotherm (Equation 5) as illustrated in Fig. 9. The value of K_{ads} and $\Delta G°_{ads}$ are listed in Table III.6. The big value of K_{ads} indicates much more efficient adsorption and hence an increase in inhibition efficiency. K_{ads} for the GDE was 0.67 L.g^{-1}, but after adding the potassium iodide, K_{ads} for GDE/iodide ions system increases up to 120.04 L.g^{-1} indicating more adsorption of the GDE on API 5L X70 pipeline steel surface. In the present study, $\Delta G°_{ads}$ of the GDE/iodide ions system is 28.97 kJ mol^{-1}, which indicates that the adsorption of the

GDE/iodide ions system on API 5L X70 pipeline steel surface involves both chemisorption and physisorption.

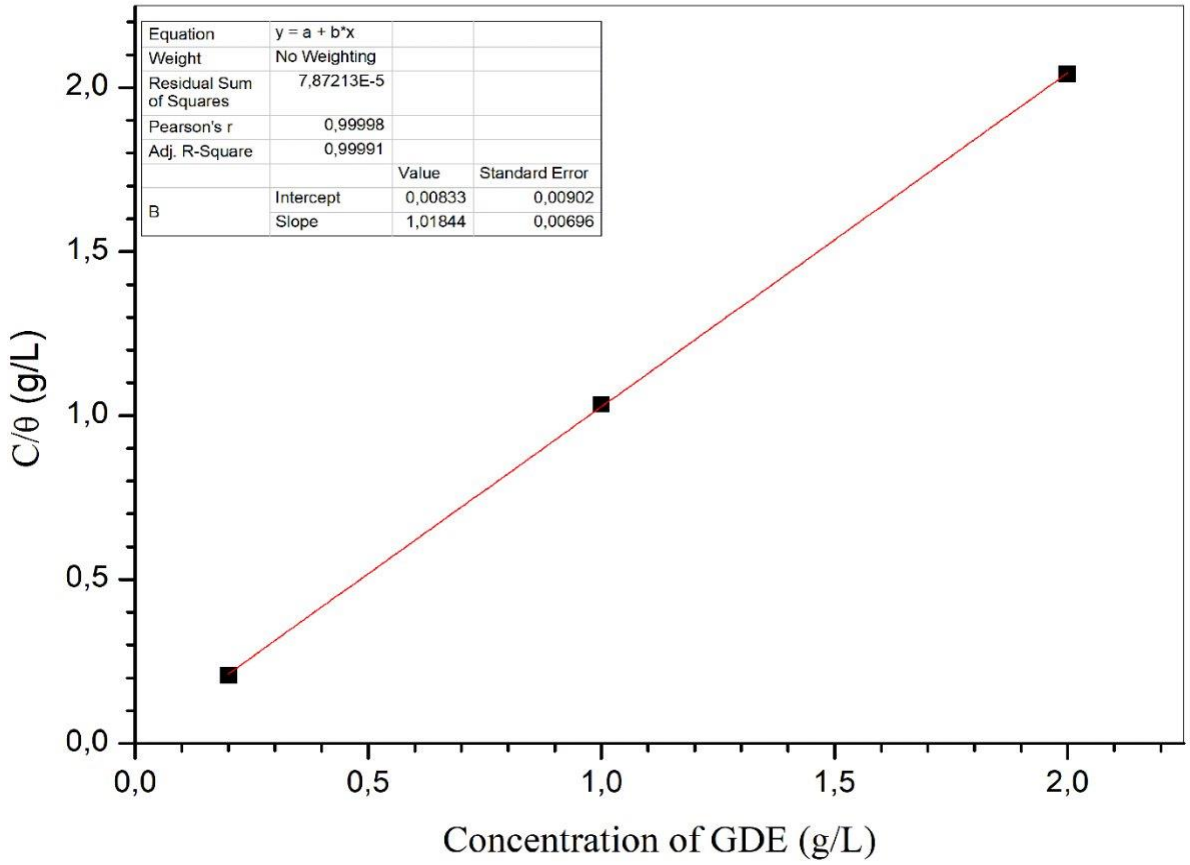

Figure III.8 7. Langmuir adsorption isotherm of API5L X70 steel in 0.5 mol.L^{-1} sulfuric acid containing 5×10^{-4} mol.L^{-1} of potassium iodide (KI) combined with different concentrations of the GDE.

Table III. 6.Langmuir adsorption isotherm parameters of API 5L X70 pipeline steel in 0.5 mol.L^{-1} sulfuric acid for the GDE/iodide ions system at 25 °C.

Isotherm mode	Linear correlation coefficient	Slope	K_{ads} (L g^{-1})	$\Delta G°_{ads}$ (kJ mol^{-1})
Langmuir	0.99998	1.018	120.04	-28.97

III.4.SEM–EDX analysis

Fig. III.9 shows the SEM images and the corresponding composition element (EDX spectra) of API 5L X70 pipeline steel surface, after 72 hours of immersion time in 0.5 mol. L^{-1} sulfuric acid without, with the GDE and GDE/iodide ions system.

When the steel was immersed in sulfuric acid, it was observed that in addition to the element iron, the element oxygen and the element sulphur are present as a consequence of the corrosion phenomenon (Fig. . III.9 a). In the SEM image corresponding to the sample with GDE (Fig. III.9 b), a reduction in corrosion is clear compared to the SEM image without the GDE (Figure . III.9 a). After adding the potassium iodide to the GDE, almost no corrosion products were observed on the API 5L X70 pipeline steel surface (Fig.III.9c).

To define the elements present in steel surface EDX analyses were utilized. In the GDE/iodide ions system, the amount of oxygen and sulphur significantly decreases. On the contrary, it is noticed that the amount of iron increases considerably (Table III.7), probably due to the adsorption of the GDE on the API 5L X70 pipeline steel surface.

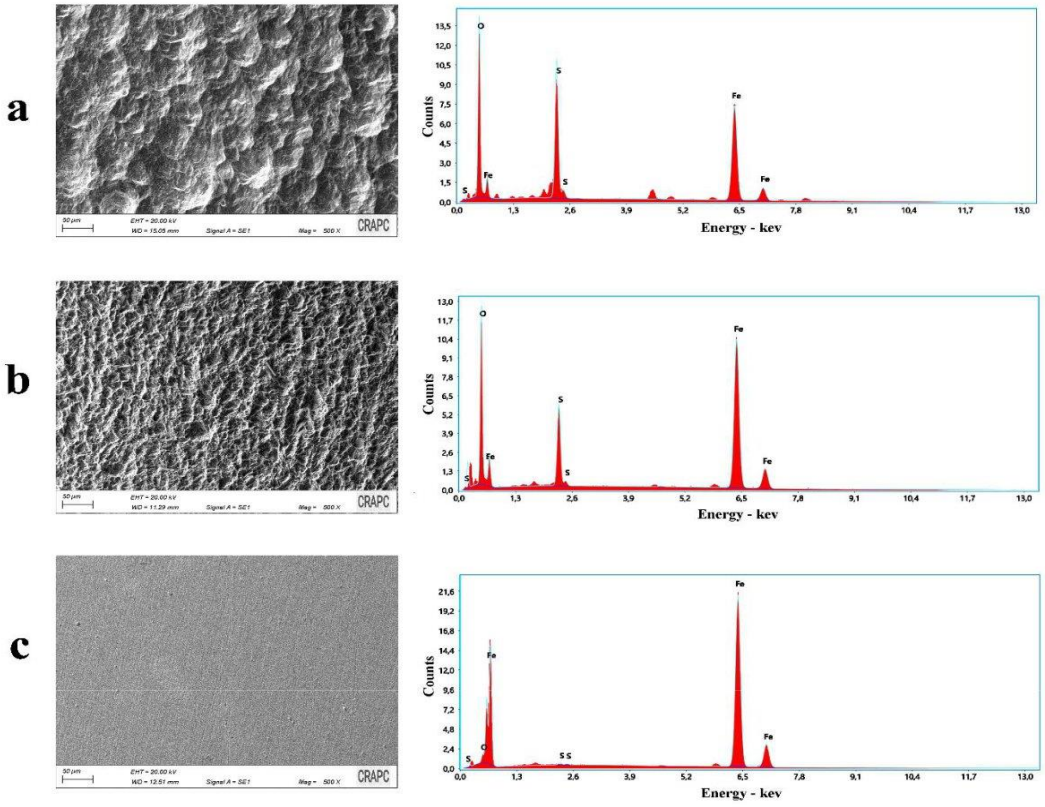

Figure III.9.SEM–EDX spectra of API5L X70 pipeline steel surface after 72 hours of immersion at 20°C: (a) 0.5M H_2SO_4, (b) 0.5M H_2SO_4 + 2 g/L GDE, (c) 0.5M H_2SO_4 + 2 $g.L^{-1}$ GDE + 0.5 mM KI.

Table III. 7.Elemental composition (% atomic) obtained from the energy-dispersive X-ray spectra for API 5L X70 pipeline steel surface, after 72 hours immersion time in 0.5 mol.L^{-1} sulfuric acid without, with the GDE and GDE/iodide ions system

Element		% atomic	
	Steel + sulfuric acid	Steel + sulfuric acid + 2 g.L^{-1} GDE	Steel + sulfuric acid + 2.g L^{-1} GDE + 0.5 x 10^{-4} mol.L^{-1} KI
iron	25.80	40.18	94.84
oxygen	56.92	49.25	4.46
Sulfur	17.28	10.06	0.70

III.5.Mechanism of corrosion inhibition

Depending on the value of standard adsorption free energy (ΔG_{ads}) and synergism parameter (S) for the GDE/iodide ions system, the inhibition mechanism can be proposed.

Iodide ions (I^-) were known to have a synergistic effect with polysaccharides (when used as corrosion inhibitors) in acid solutions.[146] The main component of polysaccharides in the GDE is galacturonic acid. In sulfuric acid, galacturonic acid molecules charge a positive charge after their protonation (Figure 10a), and with the same behaviour, the API 5L X70 pipeline steel surface is charged positively. Meanwhile, the iodide ions in the sulfuric acid can be specifically adsorbed on the steel surface, thereby making the API 5L X70 surface charge negative. Electrostatic attraction between the adsorbed I^- and protonated galacturonic acid molecules was the main driving force (physisorption) (Figure 10b). In this way, galacturonic acid molecules form a dense layer to protect the API 5L X70 pipeline steel. The function groups such as −O− in the galacturonic acid can share and donate electrons to the empty orbital of iron and form coordination bonds (chemisorption) and block the active sites of the steel surface (Figure 10b), and result in additional protection.

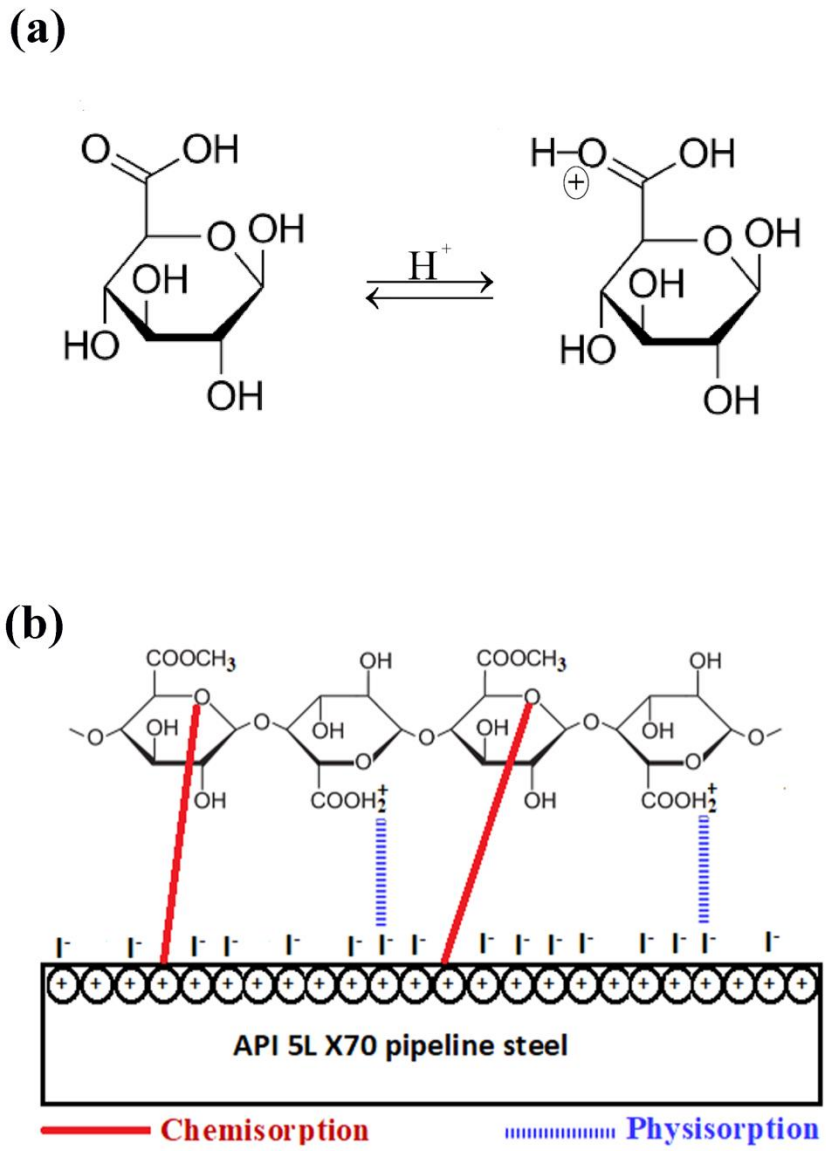

Figure III. 10. (a) Protonation of galacturonic acid, and (b) schematic illustration of the adsorption behaviour of GDE on API 5L X70 pipeline steel surface in 0.5 mol.L^{-1} sulfuric acid.

Because of the complex chemical composition of the GDE, it will be very difficult to identify the component responsible for corrosion inhibition. Therefore, some compounds of the GDE that have proven an inhibition efficiency for metals in acidic media (gallic acid.[147], apigenin.[148] , quercetin. [149] , phenolic components.[150] and many other components) cannot be neglected.

General Conclusion

General Conclusion

The aim of this thesis was to study the synergy between iodide ions and a natural compound (Ghars date extract (GDE)) proposed as a green corrosion inhibitor in sulphuric acid for the petroleum industry. For this, the inhibition efficiency of GDE and GDE/iodide ions system were determined mainly by electrochemical measurements. The inhibitor was chosen because it is characterized by: non-toxicity, biodegradability, inexpensive, and easily available from renewable sources.

The first objective of this work was mainly understanding the corrosion of API 5L X70 steel in a sulfuric acid environment and then to evaluate the synergy of KI/GDE in the acidic environment. The Nyquist representation revealed that the impedance diagram is made up in H_2SO_4 medium, of both a large capacitive loop at high frequencies and an inductive loop at low frequencies, by the SEM-EDX, showed a different corrosion morphology, while in H_2SO_4 medium, longitudinal cavities of different lengths (from 68 μm to 124 μm) were observed over the entire surface of the steel.

Then, the inhibitory properties of KI/GDE for API 5L X70 steel in H2SO4 medium were studied using electrochemical measurements and surface analyses. The SIE results revealed that a synergistic effect was observed between GDE and halides. The best synergistic effect between GDE and halide ions was found for iodide ions, The addition of iodide ions significantly increases the effectiveness

GDE inhibitory developed from 45.5% to 97.9% in 0.5 M H_2SO_4 medium. The adsorption of GDE and KI/GDE on the steel surface of the API 5L X70 pipeline in sulfuric acid medium follows the Langmuir adsorption isotherm. Potentiodynamic polarization data indicated that GDE and KI/GDE act as a mixed-type inhibitor in sulfuric acid. The adsorption standard energy ($\Delta G°_{ads}$) indicated that the adsorption of GDE involves physical adsorption. While physical and chemical adsorption is probably proposed from the trend of ($\Delta G°_{ads}$) which is more negative for KI/GDE. The SIE results indicated that in the presence of high concentrations of KI (from 0.5 mM), the inductive loop disappeared and the Nyquist diagrams for KI/GDE have only a single flattened semicircle. corresponding to a single capacitive loop. Examination of the steel surface by SEM confirms the excellent inhibitory efficiency of KI/GDE. This confirms that GDE is adsorbed on the surface of API 5L X70 steel using iodide ions. a synergistic way.

The synergy between iodide ions and Ghars date extract (GDE) resin was also studied for API 5L X70 steel in 0.5M H_2SO_4 medium by electrochemical tests and analysis of the steel surface by SEM -EDX. The SIE results showed that the inhibitory efficiency increased, for a GDE concentration equal to 2 $g.L^{-1}$, from 45.5% to 97.9% for the KI/GDE system (2$g.L^{-1}$ GDE + 5mM KI). The Nyquist representation revealed that the impedance diagram is made up in H_2SO_4 medium containing the KI/GDE system, of both a large capacitive loop at high frequencies and an inductive loop at low frequencies. The results of potentiodynamic polarization showed that the KI/RSM system decreased the corrosion rate, with a large value, from 1572 μA to 10 μA with an inhibition rate equal to 97.9%. The KI/GDE system acts as a mixed inhibitor in H_2SO_4 medium. A concentration of GDE equal to 2 $g.L^{-1}$ with 5mM KI gave a value of synergy parameter S1 equal to 2.28, which confirmed that Ghars date extract is adsorbed on the surface of API 5L X70 steel in medium H_2SO_4 using iodide ions in a synergistic manner. Analysis of the surface of API 5L X70 steel in H_2SO_4 medium by SEM-EDX revealed pitting corrosion of API 5L on the steel surface was observed. The diameter of the pits observed in the presence of GDE varies between 5 μm and 25 μm.

The mechanism of synergy proposed in this study is as follows: the iodide ions are first adsorbed, in HCl and H_2SO_4 medium, on the surface of the API 5L X70 steel, then the GDE inhibitors are associated with the iodide ion adsorbed from so that the formation of the ion pair occurs directly on the steel surface.

As perspectives, we will consider doing the following work:

- It would be more judicious to study the influence of hydrodynamic conditions, under the same operating conditions, on the effectiveness of Ghars date extract.
- It would be very useful to study the inhibitory effectiveness of Ghars date extract in other aggressive media, as well as on other metals such as copper, aluminum, etc.
- It would also be desirable for this study to use surface characterization techniques such as XPS photoelectron spectroscopy (X-Ray Photoelectron Spectroscopy) and Raman spectroscopy in order to establish with more precision the formation of corrosion products and their interaction with Ghars date extract, with the aim of improving their corrosion protection capabilities.

References

References

[1] M. Shahid, Corrosion protection with eco-friendly inhibitors, Advances in Natural Sciences: Nanoscience and Nanotechnology, 2 (2011) 043001.

[2] Y. Ma, F. Han, Z. Li, C. Xia, Acidic-Functionalized Ionic Liquid as Corrosion Inhibitor for 304 Stainless Steel in Aqueous Sulfuric Acid, ACS Sustainable Chemistry & Engineering, 4 (2016) 5046-5052.

[3] H. Taoui, H. Bentrah, A. Chala, M. Djellab, Bark resin of Schinus molle as an eco-friendly inhibitor for API 5L X70 pipeline steel in HCl medium, Materials and Corrosion, 70 (2019) 511-520.

[4] R. Haldhar, D. Prasad, I. Bahadur, O. Dagdag, A. Berisha, Evaluation of Gloriosa superba seeds extract as corrosion inhibition for low carbon steel in sulfuric acidic medium: A combined experimental and computational studies, Journal of Molecular Liquids, 323 (2021) 114958.

[5] A. Thoume, A. Elmakssoudi, D.B. Left, N. Benzbiria, F. Benhiba, M. Dakir, M. Zahouily, A. Zarrouk, M. Azzi, M. Zertoubi, Amino acid structure analog as a corrosion inhibitor of carbon steel in 0.5 M H2SO4: Electrochemical, synergistic effect and theoretical studies, Chemical Data Collections, 30 (2020) 100586.

[6] P. Rao, B.P. Charitha, , Starch as an ecofriendly green inhibitor for corrosion control of 6061-Al alloy, Journal of Materials and Environmental Science 1(2017) 78-89.

[7] H.M. Yang, Role of Organic and Eco-Friendly Inhibitors on the Corrosion Mitigation of Steel in Acidic Environments-A State-of-Art Review, Molecules (Basel, Switzerland), 26 (2021).

[8] S. Abbout, M. Zouarhi, D. Chebabe, M. Damej, A. Berisha, N. Hajjaji, Galactomannan as a new bio-sourced corrosion inhibitor for iron in acidic media, Heliyon, 6 (2020) e03574.

[9] W. Zhang, Y. Ma, L. Chen, L.-J. Wang, Y.-C. Wu, H.-J. Li, Aloe polysaccharide as an eco-friendly corrosion inhibitor for mild steel in simulated acidic oilfield water: Experimental and theoretical approaches, Journal of Molecular Liquids, 307 (2020) 112950.

[10] S.C. Nwanonenyi, H.C. Obasi, I.C. Chukwujike, M.A. Chidiebere, E.E. Oguzie,

Inhibition of Carbon Steel Corrosion in 1 M H2SO4 Using Soy Polymer and Polyvinylpyrrolidone, Chemistry Africa, 2 (2018) 277-289.

[11] A. Biswas, S. Pal, G. Udayabhanu, Experimental and theoretical studies of xanthan gum and its graft co-polymer as corrosion inhibitor for mild steel in 15% HCl, Applied Surface Science, 353 (2015) 173-183.

[12] M. Mobin, M. Rizvi, L.O. Olasunkanmi, E.E. Ebenso, Biopolymer from Tragacanth Gum as a Green Corrosion Inhibitor for Carbon Steel in 1 M HCl Solution, ACS omega, 2 (2017) 3997-4008.

[13] M.M. Solomon, S.A. Umoren, I.I. Udosoro, A.P. Udoh, Inhibitive and adsorption behaviour of carboxymethyl cellulose on mild steel corrosion in sulphuric acid solution, Corrosion Science, 52 (2010) 1317-1325.

[14] K.C.d.S.d. Lima, V.M. Paiva, D. Perrone, B. Ripper, G. Simões, M.L.M. Rocco, A.G.d. Veiga, E. D'Elia, Glycine max meal extracts as corrosion inhibitor for mild steel in sulphuric acid solution, Journal of Materials Research and Technology, 9 (2020) 12756-12772.

[15] M. Djellab, H. Bentrah, A. Chala, H. Taoui, Synergistic effect of halide ions and gum arabic for the corrosion inhibition of API5L X70 pipeline steel in H2SO4, Materials and Corrosion, 70 (2019) 149-160.

[16] M.I. Hussain, M. Farooq, Q.A. Syed, Nutritional and biological characteristics of the date palm fruit (Phoenix dactylifera L.) – A review, Food Bioscience, 34 (2020) 100509.

[17] N.A. AlFaris, J.Z. AlTamimi, F.A. AlGhamdi, N.A. Albaridi, R.A. Alzaheb, D.H. Aljabryn, A.H. Aljahani, L.A. AlMousa, Total phenolic content in ripe date fruits (Phoenix dactylifera L.): A systematic review and meta-analysis, Saudi Journal of Biological Sciences, 28 (2021) 3566-3577.

[18] M. Elleuch, S. Besbes, O. Roiseux, C. Blecker, C. Deroanne, N.-E. Drira, H. Attia, Date flesh: Chemical composition and characteristics of the dietary fibre, Food Chemistry, 111 (2008) 676-682.

[19] M. Khatib, A. Al-Tamimi, L. Cecchi, A. Adessi, M. Innocenti, D. Balli, N. Mulinacci, Phenolic compounds and polysaccharides in the date fruit (Phoenix dactylifera L.): Comparative study on five widely consumed Arabian varieties, Food Chem, 395 (2022)

133591.

[20] M. Bammou, K. Sellam, M. Benlyas, C. Alem, Y. Filali-Zegzouti, Evaluation of antioxidant, antihemolytic and antibacterial potential of six Moroccan date fruit (Phoenix dactylifera L.) varieties, Journal of King Saud University-Science, 28 (2016) 136-142.

[21] F.M.M. Lemine, M.V.O.M. Ahmed, L.B.M. Maoulainine, Z.e.A.O. Bouna, A. Samb, A.O.M.S.O. Boukhary, Antioxidant activity of various Mauritanian date palm (Phoenix dactylifera L.) fruits at two edible ripening stages, Food science & nutrition, 2 (2014) 700.

[22] S. Ghnimi, S. Umer, A. Karim, A. Kamal-Eldin, Date fruit (Phoenix dactylifera L.): An underutilized food seeking industrial valorization, NFS journal, 6 (2017) 1-10.

[23] S. Zihad, S.J. Uddin, N. Sifat, F. Lovely, R. Rouf, J.A. Shilpi, B.Y. Sheikh, U. Göransson, Antioxidant properties and phenolic profiling by UPLC-QTOF-MS of Ajwah, Safawy and Sukkari cultivars of date palm, Biochemistry and biophysics reports, 25 (2021) 100909.

[24] Y. Li, W. Xu, J. Lai, S. Qiang, Inhibition Effect and Mechanism Explanation of Perilla Seed Extract as a Green Corrosion Inhibitor on Q235 Carbon Steel, Materials, 15 (2022).

[25] S.J. Keny, A.G. Kumbhar, C. Thinaharan, G. Venkateswaran, Gallic acid as a corrosion inhibitor of carbon steel in chemical decontamination formulation, Corrosion Science, 50 (2008) 411-419.

[26] F.S. de Souza, A. Spinelli, Caffeic acid as a green corrosion inhibitor for mild steel, Corrosion Science, 51 (2009) 642-649.

[27] A. Borchers, T. Pieler, Programming pluripotent precursor cells derived from Xenopus embryos to generate specific tissues and organs, Genes, 1 (2010) 413-426.

[28] M. Faci, Typology and varietal biodiversity of date palm farms in the North-East of Algerian Sahara, Journal of Taibah University for Science, 13 (2019) 764-771.

[29] 1.A.F. S. Abdul Rahiman, S. Sethumanickam,Corrosion inhibition,adsorption and thermodynamic properties of poly(vinyl alcohol-cysteine) in molar HCl, Arabian Jornal of Chemistry. 2017, Vol 10, pages S3358-S3366

[30]P. Mourya, S. Banerjee, M. M. Singh,Corrosion inhibition of mild steel in acidic solution by Tagetes erecta (Marigold Flower) Extract as a Green inhibitor. Corros. Sci. 2014, 85, 352-363.

[31]M. A. Zavareh , A. A Sarhan, D. M., Abd Razak, B. B., Basirun, W. J. (2014). Plasma thermal spray of ceramic oxide coating on carbon steel with enhanced wear and corrosion resistance for oil and gas applications. Ceramics International, 40(9), 14267-14277.

[32]L. S.Barreto, , M. S. Tokumoto, I. C. Guedes , H. G. D. Melo, , Amado, F. D. R., & Capelossi, V. R. (2017). Evaluation of the anticorrosion performance of peel garlic extract as corrosion inhibitor for ASTM 1020 carbon steel in acidic solution. Matéria (Rio de Janeiro), 22.

[33]S.S. Prabha, , R.J. Rathish, and R. Dorothy, CORROSION PROBLEMS IN PETROLEUM INDUSTRY AND THEIR SOLUTION. European Chemical Bulletin, 2014. 3: p. 300-307

[34]P. B. Salunkhe, , & S. P. Rane, (2016). Treatise on conducting polymers for corrosion protection–Advanced approach. Paint India, 61.

[35]P. Hopkins (2007), "Pipeline stream, past, present, and future' from the 5th Asian Pacific IIW international congress". Sydney, Australia, Key note paper.

[36]F. Grimpe, H. Meuser, F. Gerdemann, E. Muthmann (2010), "2nd International conference on Super-High Strength Steel". Peschiera Del Garda, Italy.

[37]H. G. Hillenbrand, K. A. Niederhoff, E. Amoris, C. Perdrix, , A. Streisselberg and U.Zeislmair (1997), "Development of Linepipe in Grades up to X-100". EPRG/PRC Biennial Joint Technical Meeting on Linepipe Research, Washington, D. C.

[38]J.I. Omale. (2016), "Microstructure and Mechanical properties of welds in pipeline steel", 18-21, 28-31, 100-116. M.sc Thesis, University of Saskatchewan

[39]C.M. Spinelli and L. Prandi, 7th pipeline technology conference 2012.

[40]M. Heydari and M. Javidi, Corrosion inhibition and adsorption behavior of an amido-imidazoline derivative on API4LX52 steel in CO_2 – saturated solution and synergistic effect of iodide ions. Corros. Sci.,Vol 61 (2012) page 148-155.

[41]D. Belato Rosado, W. De Waele, D. Vanderschueren and S. Hertele, J. Sustain. Constr. & Design, 2013.

[42]J.Y. Koo, M.J. Luton, N.V. Banguru, R.A. Petkovic, D. Fairchild, C.W. Petersen, H. Asahi, T. Hara, Y. Terada, M. Sugiyama, H. Tamehiro, Y, Komizo, S. Okaguchi, M. Hamada, A. Yamamoto and I. Takeuchi, Proceedings of 13th international offshore and polar engineering

conference, Honolulu, Hawaii, USA, 2003.

[43] M. A. J. Mazumder, H. A. Al-Muallem and S. A. Ali,The effect of N-pendants and electron-richamidine motifs in 2-(p-alkoxyphenyl)-2-imidazolines on mild steel corrosion in CO_2-saturated 0.5M NaCl.Corros. Sci., Vol90 (2015) page 54-68.

[44] M. A. Gough, W.H. Durnie, E.K. Auty and B. Hedges, Corrosion 2002, Paper No. 02301.

[45] E. M.Genies, , Boyle, A., M. Lapkowski, , and C. Tsintavis (1990): Polyaniline: A his- torical survey, Synth. Met., Vol36(2). page 139-182.

[46] L. Garverick, Corrosion in the Petrochemical Industry. 1994: ASM International.

[47] J. R. Davis, Corrosion: Understanding the Basics. 2000: A S M International.

[48] A.Singh, , & M. A.Quraishi,. (2015). Acidizing corrosion inhibitors: a review. J. Mater. Environ. Sci, 6(1), 224-235.

[49] B. Little, P. Wagner, F. Mansfeld, Microbiologically influenced corrosion of metals and alloys. International Materials Reviews, (1991). 36(1): p. 253-272.

[50] J. R. Davis, *Corrosion: Understanding the Basics*. **2000**: ASM International

[51] Bohni, H., and H.H. Uhlig , Environmental Factors Affecting the Critical Pitting Potential of Aluminum J. Electrochem Soc, Vol 116,Number 7, 1969.

[52] R.Baboian, , et al., "Galvanic and Pitting Corrosion - Field and Laboratory Studies," ASTM STP 576,p 5-19 American Society for Testing and Materials, 1974.

[53] W.K. Boyd,. and F.W. Fink, "Corrosion of Metals in Marine Environments," Battelle Columbus Laboratories, MCIC-78-37, 1978.

[54] H.H. Uhlig,. and R.W. Revie, Corrosion and Corrosion Control, 3rd, ed., Wiley-Interscience, NY, 1985.

[55] J.G. Speight, *Rules of thumb for petroleum engineers*. 2017: John Wiley & Sons.

[56] H. Bentrah , A. CHALA, (2015). Corrosion des ouvrages pétroliers : Utilisation de la gomme arabique comme inhibiteur environnemental pour l'acier API 5L X42. *Université Mohamad Khider, BISKRA, Doctorat*.

[57] M.L. Brusseau , J. Chorover, (2019). Chemical processes affecting contaminant transport and fate. In *Environmental and Pollution Science* (pp. 113-130). Academic Press

[58] L. M. Alcalá, (2012). Acid stimulation of geothermal wells in Mexico, El Salvador and The Philippines. REVISTA MEXICANA DE GEOENERGÍA· ISSN 0186 5897, 17.

[59] M. Al-Mahasneh, , S. Al Rabadi , H. Khaswaneh, (2021). Assessment of oil-producing wells by means of stimulation approach through matrix acidizing: a case study in the Azraq region. Journal of Petroleum Exploration and Production Technology, 11(9),

3479-3491.

[60] M. U. Shafiq , H. B. Mahmud, (2017). Sandstone matrix acidizing knowledge and future development. Journal of Petroleum Exploration and Production Technology, 7(4), 1205-1216.

[61] A. Hamdy, N.S. El-Gendy,Thermodynamic, adsorption and electrochemical studies for corrosion inhibition of carbon steel by henna extract in acid medium Egyptian Petroleum Research Institute, Nasr City 11727, Cairo, Egypt Received 14 May 2012; accepted 19 June 2012

[62] V. V. Torres, R. S. Amadoa, C. Faia de Saa, T. L. Fernandez a, C. A. da Silva Riehlb, A. G. Torresc, E. D'Elia, Inhibitory action of aqueous coffee ground extracts on the corrosion of carbon steel in HCl solution aDepartamento de Quimica Inorganica, Instituto de Quimica, UFRJ, Avenida Athos da Silveira Ramos 149, Centro de Tecnologia, Bloco A - Laboratorio 634A, CEP 21941-909, Cidade Universitaria, Rio de Janeiro, RJ, Brazil

[63] A. El Bribri, M. Tabyaoui,1, B. Tabyaouia, H. El Attaric, F. Bentissc ,The use of Euphorbia falcata extract as eco-friendly corrosion inhibitor of carbon steel in hydrochloric acid solution , Laboratoire de Chimie Organique, Bioorganique et Environnement, Faculte des Sciences, Universite Chouaib Doukkali, B.P. 20, M-24000 El Jadida, Morocco Materials Chemistry and Physics xxx(2013)1-8

[64] H. Taoui, H. Bentrau, A. Chala, M. Djellab. Bark resin of Schinus molle as an eco-friendly inhibitor for API 5L X70 pipeline steel in HCl medium. ARTICLE Materials and Corrosion ,DOI: 10.1002/maco.201810477 , Received: 12 August 2018, Accepted: 17 September 2018.Journal MACO , MSP No. 201810477

[65] M.Bobinaa, A. Kellenbergera, J. P. Milletb, C. Munteana, N. Vaszilcsin, Corrosion resistance of carbon steel in weak acid solutions in the presence of L-histidine as corrosion inhibitor University Politehnica of Timisoara, Piata Victoriei 2, 300006 Timisoara, Romania b University of Lyon, INSA-Lyon, MATEIS - CNRS UMR 5510, F69621 Villeurbanne Cedex, France , Corrosion Science 69 (2013) 65-395

[66] A.Abdel Nazeer , K. Shalabi , A. S. Fouda, Corrosion inhibition of carbon steel by Roselle extract in hydrochloric acid solution: electrochemical and surface study 18

February 2014, Springer Science+Business Media Dordrecht 2014 .

[67]M. Aliofkhazraei, (Ed.). (2014). *Developments in corrosion protection*. BoD–Books on Demand

[68]D. Kesavan , M. Gopiraman, and N. Sulochana, Green Inhibitors for Corrosion of Metals A Review. Chemical Science Review and Letters, 2012: p. 1-8

[69]L. S.Barreto, , M. S.Tokumoto , I. C. Guedes , H. G. D. Melo, , F. D. R. Amado, V. R. Capelossi, (2017). Evaluation of the anticorrosion performance of peel garlic extract as corrosion inhibitor for ASTM 1020 carbon steel in acidic solution. *Matéria (Rio de Janeiro), 22*.

[70]I. Nadi et al, Sargassum muticum extract based on alginate biopolymer as a new efficient biological corrosion inhibitor for carbon steel in hydrochloric acid pickling environment: Gravimetric, electrochemical and surface studies. International Journal of Biological Macromolecules, 2019. 141: p. 137-149.

[71]F. Ropital, , Corrosion and degradation of metallic materials. 2010: Editions Technip.

[72]P. Gupta, R. S. Chaudhary, T. K. G. Namboodhiri, B. Prakash, and B. B. Prasad, *Corros. Sci*, 40 (1984) 33-36.

[73]A. Chaouiki, et al, *Understanding corrosion inhibition of mild steel in acid medium by new benzonitriles: Insights from experimental and computational studies.* Journal of Molecular Liquids, 2018. **266**: p. 603-616.

[74]C. Erkey , Thermodynamics and Dynamics of Adsorption of Metal Complexes on Surfaces from Supercritical Solutions. 2011. 1: p. 41-77.

[75]E. Mccafferty , Introduction to Corrosion Science. Springer, 2010.

[76]E. Ituen , O. Akaranta, A. James, (2017). Evaluation of performance of corrosion inhibitors using adsorption isotherm models: an overview. *Chem. Sci. Int. J*, *18*(1), 1-34.

[77]I. Nadi et al., Sargassum muticum extract based on alginate biopolymer as a new efficient biological corrosion inhibitor for carbon steel in hydrochloric acid pickling environment: Gravimetric, electrochemical and surface studies. International Journal of Biological Macromolecules, 2019. 141: p. 137-149.

[78]V. M. Abbasov, A. El-Lateef, H. M, Aliyeva, L. I, Qasimov, E. E, Ismayilov, I. T, M. M. Khalaf, (2013). A study of the corrosion inhibition of mild steel C1018 in CO2-saturated brine using some novel surfactants based on corn oil. *Egyptian Journal of Petroleum*, *22*(4), 451-470.

[79]L. Lia, X.Zhang a, J. Leia, J.Hea, S. Zhang a, F. Panb, Adsorption and corrosion

inhibition of Osmanthus fragran leaves extract on carbon steel ,Corrosion Science.Vol. 63 October(2012) 67-90

[80]M. Messali , et al, Guar gum as efficient non-toxic inhibitor of carbon steel corrosion in phosphoric acid medium: Electrochemical, surface, DFT and MD simulations studies. Journal of Molecular Structure, 2017. 1145: p. 43-54.

[81]L. Afia , O. Benali, R. Salghi ' , Eno. E. Ebenso ' , S. Jodeh , M. Zougagh , B. Hammouti Steel Corrosion Inhibition by Acid Garlic Essential Oil as a Green Corrosion Inhibitor and Sorption Behavior . Int. J. Electrochem. Sci., 9 (2014) 8392 - 8406

[82]L. S. Barreto, , M. S.Tokumoto , I. C. Guedes, H. G. D. Melo, F. D. R. Amado, V. R. Capelossi, (2017). Evaluation of the anticorrosion performance of peel garlic extract as corrosion inhibitor for ASTM 1020 carbon steel in acidic solution. Matéria (Rio de Janeiro), 22.

[83]H. TAOUI, (2020). Protection against corrosion of API 5L X70 carbon steel intended to petroleum industry by green inhibitor: SchinusMolle Resin as an eco-friendly inhibitor (Doctoral dissertation, Université Mohamed Khider–Biskra).

[84]R. Bhaskaran, N. Palaniswamy, N.S. Rengaswamy and M. Jayachandran, A review of differing approaches used to estimate the cost of corrosion (and their relevance in the development of modern corrosion prevention andp control strategies) Anti-Corr.Methods Mater., V 52 (2005) P 29-41

[85]R. Narayan, "An introduction to metallic corrosion and its prevention" Oxford Publishing Company, New Delhi (1990).

[86]J. Nie, Improvements in the Use of Mg Pigments in Corrosion Protective Coatings, Fargo: UMI Dissertation Publishing, 2010.

[87]H. Elabbasy, S. Zidan, and A. El-Aziz, *Inhibitive behavior of Ambrosia Maritima extract as an eco-friendly corrosion inhibitor for carbon steel in 1M HCl.* Zastita materijala, 2019. **60**(2): p. 129-146.

[88]S. Garaia, S. Garaib, P. Jaisankarb, J.K. Singhc, A. Elangod A comprehensive study on crude methanolic extract of Artemisia pallens (Asteraceae) and its active component as effective corrosion inhibitors of mild steel in acid solution Corrosion Science 60 (2012) 67-204

[89]M.Salasia, T. Shahrabia, E. Roayaeib, M. Aliofkhazraeia, The electrochemical behaviour of environment-friendly inhibitors of silicate and phosphonate in corrosion control of carbon steel in soft water media, Materials Chemistry and Physics 104(2007)

183-190

[90] D. Sarada Kalyani , S. Srinivasa , M. Sarath Babu , B.V.Appa Rao, B.Sreedhar. Electrochemical and surface analytical studies of carbon steel protected from corrosion in a law – chloride environment containing a phosphonate-based inhibitor. Res Chem Intermed , DOI 10.1007/s11164-014-1584-y

[91] A.M. Ruiz, et al, Opuntia ficus-indica (Nopal Extract) as Green Inhibitor for Corrosion Protection in Industrial Steels. Corrosion Inhibitors, Principles and Recent Applications, 2018: p. 145.

[92] *C. Abdelkarim, et al. "Understanding corrosion inhibition of mild steel in acid medium by new benzonitriles: insights from experimental and computational studies." Journal of Molecular Liquids 266 (2018): 603-616*

[93] P.Gupta, R.S, Chaudharym T.K.G, Namboodhiri, B. Parkash, and B.B. Prasad, Corras, Sci.40 (1984)33-36.

[94] H. Bentrah , et al., The influence of temperature on the corrosion inhibition of API 5L X42 pipeline steel in HCl medium by gum arabic. Anti-Corrosion Methods and Materials, 2017. 4: p. 409-417.

[95] Z. Shahnavaz, W. J. Basirun, S. M. Zain, *Anti Corr MethMater* 2010; 57: 21-27.

[96] M. Djellab , H. Bentrah , A. Chala , H. Taoui, Synergistic effect of halide ions and gum arabic for the corrosion inhibition of API5L X70 pipeline steel in H2SO4 , DOI: 10.1002/maco.201810203.

[97] J.-B. Perez-Navarrete ,Establishment of Electrical Equivalent Circuits from Electrochemical Impedance Spectroscopy Study of Corrosion Inhibition of Steel by Imidazolium Derived Ionic Liquids in Sulphuric Acidic Solution , 2010 7th International Conference on Electrical Engineering, Computing Science and Automatic Control (CCE 2010) Tuxtla Gutierrez, Chiapas, Mexico. September 8-10, 2010.., Mexico

[98] R. Naderi,, S.Y. Arman b, Sh. Fouladvandb , Investigation on the inhibition synergism of new generations of phosphate-based anticorrosion pigments , Dyes and Pigments 105 (2014) 68—33.

[99] S. Srinivasa Rao1 , B.V. Appa Rao, S. Roopas Kiran, B. Sreedhar, Lactobionic Acid as a New Synergist in Combination with Phosphonate-Zn(II) System for Corrosion Inhibition of Carbon Steel, J. Mater. Sci. Technol., 2014, 30(1), 77-89.

[100] AS. Yaro, A.A. Khadom, R.K. Wael. Apricot juice as green corrosion inhibitor of

mild steel in phosphoric acid. Alex Eng J. 2013;52:129-35.

[101] S. A. Umoren, M. M. Solomon, *Synergistic corrosion inhibition effect of metal cations and mixtures of organic compounds: A Review.* Journal of Environmental Chemical Engineering, **2017**. **5**: p. 246-273.

[102] M. Chigondo, F. Chigondo, (2016). Recent natural corrosion inhibitors for mild steel: an overview. Journal of Chemistry, 2016.

[103] O. K. Abiola, J. O. E. Otaigbe, O. J. Kio, Gossipium hirsutum L, *Corros. Sci.,* 59 (2009) 1879-1881.

[104] S.A. Umoren, I.B. Obot, E.E. Ebenso, N.O. Obi-Egbedi. The Inhibition of aluminium corrosion in hydrochloric acid solution by exudate gum from Raphia hookeri. Desalination 2009;Vol 247 Issues (1-3) 561-572

[105] Z.X.Tang, L.E. Shi, S.M. Aleid (2013) Date fruit: chemical composition, nutritional and medicinal values, products. J Sci Food Agric 93:2351–2361. https://doi.org/10.1002/jsfa.6154

[106] A.A. Abul-Soad, Jain SM, Jatoi MA (2017) Biodiversity and conservation of date palm. In: Ahuja MR, Jain SM (eds) Biodiversity and conservation of woody plants, Sustainable development and biodiversity, vol 17. Springer, Cham, pp 313–353

[107] A. El Hadrami, J.M. Al-Khayri, (2012) Socioeconomic and traditional importance of date palm.Emir J Food Agric 24:371–385

[108] M.A. Al-Farsi, C.Y Lee, (2008) Nutritional and functional properties of dates: a review. Crit Rev Food Sci Nutr 48:877–887. https://doi.org/10.1080/10408390701724264

[109] M. Al-Farsi, C. Alasalvar, M. Al-Abid, K. Al-Shoaily, M. Al-Amry, F. Al-Rawahy (2007) Compositional and functional characteristics of dates, syrups and their by-products. Food Chem 104:943–947. https://doi.org/10.1016/j.foodchem.2006.12.051

[110] C. Zhang, S.A. Aldosari, P. Vidyasagar, P. Shukla, MG. Nair, (2015) Determination of the variability of sugars in date fruit varieties. J Plant Crops 43:53–61

[111] J .Ahmed, F.M, Al-Jasass, M, Siddiq (2013) Date fruit composition and nutrition. In: Siddiq M, Aleid SM, Kader AA (eds) Dates: postharvest science, processing technology and health benefits. Wiley, Chichester, pp 261–283

[112] W, Al-Shahib, R.J, Marshall, (2003) The fruit of the date palm: it's possible use as the best food for the future? Int J Food Sci Nutr 54:247–259. https://doi.org/10.1080/09637480120091982

[113] N. Chaira, A. Mrabet, A. Ferchichi (2009) Evaluation of antioxidant activity, phenolics, sugar and mineral contents in date palm fruits. J Food Biochem 33:390–403. https://doi.org/10.1111/j.1745-4514.2009.00225.x

[114] M. Shafiei, K. Karimi, M.J. Taherzadeh (2010) Palm date fibers: analysis and enzymatic hydrolysis. Int J Mol Sci 11:4285–4296. https://doi.org/10.3390/ijms11114285

[115] A. Rohani, Date paim; Tehran University Publication Center, Tehran, Iran, 1988; pp.292.

[116] P.K. Vayalil, (2014) Bioactive compounds, nutritional and functional properties of date fruit. In: Siddiq M, Aleid SM, Kader AA (eds) Dates: postharvest science, processing technology and health benefits. Wiley, Chichester, pp 285–303. https://doi.org/10.1002/9781118292419.ch12

[117] M. Al-Farsi, C. Alasalvar, A. Morris, M. Baron, F. Shahidi (2005) Comparison of antioxidant activity, anthocyanins, carotenoids, and phenolics of three native fresh and sun-dried date (Phoenix dactylifera L.) varieties grown in Oman. J Agric Food Chem 53:7592–7599. https:// doi.org/10.1021/jf050579q

[118] E.T. Bouhlali, M. Ramchoun, C. Alem, K. Ghafoor, J .Ennassir, Y.F. Zegzouti (2017) Functional composition and antioxidant activities of eight Moroccan date fruit varieties (Phoenix dactylifera L.). J Saudi Soci Agri Sci 16:257–264. https://doi.org/10.1016/j.jssas.2015.08.005

[119] M.Hashempoor, Date Treasure; Agricultural Education Publication: Tehran, Iran, 1999; pp.668

[120] A.Rohani, Date palm; Tehran University Publication Center: Tehran, Iran, 1988; pp.292

[121] M. A. Malik, M. A. Hashim, F. Nabi, Shaeel. Ahmed. AL-Thabaiti, and Z. Khan, Anti-corrosion Ability of Surfactants. 2011. 6: p. 1927 - 1948.

[122] H. Bentrah, Y. Rahali, and A. Chala, Gum Arabic as an eco-friendly inhibitor for API 5L X42 pipeline steel in HCl medium. Corrosion Science, 2014. 82: p. 426-431

[123] K.Z. Mohammed, A. Hamdy, A. Abdel-wahab, and N. A. Farid, Temperature Effect on Corrosion Inhibition of Carbon Steel in Formation Water by Non-ionic Inhibitor and Synergistic Influence of Halide Ions. 2012. 9: p. 424-434.

[124] X. Li, L. Tang, G. Mu, L. Li, and G. Liu, The synergistic inhibition of the cold rolled steel Corrosion in 0.5 M sulfuric acid by the mixture of OP and bromide ion.

Materials Letters, 2007. 61: p. 2723-2727.

[125] X. Li and L. Tang, Synergistic inhibition between OP and NaCl on the corrosion of cold-rolled steel in phosphoric acid. Materials Chemistry and Physics, 2005. 90: p. 286-297.

[126] M. Khatib, A. Al-Tamimi, L. Cecchi, A. Adessi, M. Innocenti, D. Balli, N. Mulinacci, *Food Chem.* **2022**, *395*, 133591.

[127] A. H. Al-Moubaraki, *Chem. Eng. Commun.* **2014**, *202*, 1069

[128] R. A. Al-Alawi, J. H. Al-Mashiqri, J. S. M. Al-Nadabi, B. I. AlShihi, Y. Baqi, *Front. Plant Sci.* **2017**, *8*, 8.

[129] M. Chylińska, M. Szymańska-Chargot, A. Zdunek, Carbohydr. Polym. 2016, 154, 48-54.

[130] T.-T. Chen, Z.-H. Zhang, Z.-W. Wang, Z.-L. Chen, H. Ma, J.-K. Yan, Food Hydrocolloids. 2021, 2021 v.113, pp. 106484-.

[131] G. Zhao, J. Kan, Z. Li, Z. Chen, Carbohydr. Polym. 2005, 61, 125-131.

[132] I. Trigui, H. Yaich, A. Sila, S. Cheikh-Rouhou, A. Bougatef, C. Blecker, H. Attia, M. A. Ayadi, Int. J. Biol. Macromol. 2018, 117, 937-946.

[133] A. Mokni Ghribi, A. Sila, I. Maklouf Gafsi, C. Blecker, S. Danthine, H. Attia, A. Bougatef, S. Besbes, Int. J. Biol. Macromol. 2015, 75, 276-282.

[134] S. A. Umoren, I. B. Obot, J. Adhes. Sci. Technol. 2014, 28, 2054-2068.

[135] M. Lebrini, M. Lagrenée, H. Vezin, M. Traisnel, F. Bentiss, Corros. Sci. 2007, 49, 2254-2269.

[136] M. Cui, S. Ren, Q. Xue, H. Zhao, L. Wang, J. Alloys Compd. 2017, 726, 680-692.

[137] B. Qian, J. Wang, M. Zheng, B. Hou, Corros. Sci. 2013, 75, 184-192.

[138] H. Shamsuddeen, U. Saviour, A. Shaikh, S. Moses, Int. J. Electrochem. Sci. 2017, 9061-9083.

[139] G. Sığırcık, D. Yildirim, T. Tüken, Corros. Sci. 2017, 120, 184-193.

[140] Y. Qiang, S. Zhang, S. Yan, X. Zou, S. Chen, Corros. Sci. 2017, 126, 295-304.

[141] K. Ghulamullah, J. Wan, Basirun, B. Ahmed, Bin Mohamad, Badry, N. Salim, Kazi, A. Pervaiz, M. Syed, Ahmed, M. Ghulam, Khan, Int. J. Electrochem. Sci. 2018, 13, 12420 – 12436.

[142] N. Soltani, N. Tavakkoli, M. Khayatkashani, M. R. Jalali, A. Mosavizade, Corros. Sci. 2012, 62, 122-135.

[143] G. Salinas-Solano, J. Porcayo-Calderon, L. M. Martinez de la Escalera, J. Canto,

M. Casales-Diaz, O. Sotelo-Mazon, J. Henao, L. Martinez-Gomez, Industrial Crops and Products. 2018, 119, 111-124.

[144] M. M. Solomon, S. A. Umoren, A. U. Israel, I. G. Etim, Pigm. Resin Technol. 2016, 45, 280-293.

[145] L. Zhang, Y. He, Y. Zhou, R. Yang, Q. Yang, D. Qing, Q. Niu, Petroleum. 2015, 1, 237-243.

[146] P. Muthukrishnan, B. Jeyaprabha, P. Prakash, Arab. J. Chem. 2017, 10, S2343-S2354.

[147] M. Djellab, H. Bentrah, A. Chala, H. Taoui, S. Kherief, B. Bouamra, Mater. Corros. 2020, 71, 1276-1288.

[148] X. Zhang, W.-F. Jiang, H.-L. Wang, C. Hao, J. Adhes. Sci. Technol. 2019, 33, 736-760.

[149] D. Sukul, A. Pal, S. K. Saha, S. Satpati, U. Adhikari, P. Banerjee, Phys. Chem. Chem. Phys. 2018, 20, 6562-6574.

[150] T. Sithuba, N. D. Masia, J. Moema, L. C. Murulana, G. Masuku, I. Bahadur, M. M. Kabanda, Results Eng. 2022, 16, 100694.

Abstract:

Ghars date fruit is very rich in polysaccharides, which qualifies it to be exploited as a green corrosion inhibitor. Ghars date is produced in large commercial quantities in Africa and Asia, which gives them the opportunity to be used as a cheap raw material for the industry of eco-friendly inhibitors. The synergy between the Ghars date extract (GDE) and iodide ions is investigated for the first time to improve the inhibition efficiency for API 5L X70 pipeline steel in 0.5 mol L^{-1} sulfuric acid. The synergistic effect of the GDE and iodide ions is studied by potentiodynamic polarization curves and electrochemical impedance spectroscopy, scanning electron microscopy (SEM) and energy-dispersive X-ray spectroscopy (EDX). The inhibition efficiency is 45.5 % at 2 g L^{-1} GDE at 20 °C, while it increases to 97.9 % when 5×10^{-4} mol L^{-1} of potassium iodide is added at 25 °C. It is found that significant corrosion inhibition can be obtained in a synergistic manner. The GDE/iodide ion system follows the Langmuir adsorption isotherm, involves both physical adsorption and chemical adsorption and acts as a mixed-type inhibitor.

Keywords: chemisorption; date palm fruits; green corrosion inhibitors; galacturonic acid; pipeline steels; physisorption; sulfuric acid; synergistic effect

Résumé:

La synergie entre l'Extrait de Dattes de Ghars (EDG) et les ions iodure a été étudiée pour la première fois afin d'améliorer l'efficacité d'inhibition de l'acier de pipeline API5L X70 dans de l'acide sulfurique à 0,5 M. L'effet synergique du EDG et des ions iodure a été étudié à l'aide de courbes de polarisation potentiodynamiques et de spectroscopie d'impédance électrochimique, de Microscopie Electronique à Balayage (MEB) et de spectroscopie à rayons X à Dispersion d'Energie (XDE). L'efficacité d'inhibition était de 45,5 % à 2 g/L de EDG à 20 °C, tandis qu'elle atteignait 97,9 % lorsque 0,5 mM de KI était ajouté à 25 °C. Il a été constaté qu'une importante inhibition de la corrosion pouvait être obtenue de manière synergique. Le système EDG/ion iodure suit l'isotherme d'adsorption de Langmuir, impliquant à la fois une adsorption physique et une adsorption chimique, et agit comme un inhibiteur de type mixte.

Mots-clés : Acier de pipeline ; Acide sulfurique ; Inhibiteur de corrosion écologique ; Fruit du palmier-dattier ; Acide galacturonique ; Physisorption ; Chimisorption ; effet synergique

ملخص:

تعتبر فاكهة تمور الغرس غنية جدًا بالعديد من السكريات، وهذا ما يجعلها قابلة للاستغلال كمانع طبيعي للتآكل. حيث يتم إنتاج تمور الغرس بكميات تجارية كبيرة في إفريقيا وآسيا ، وهذا ما يخولها للاستخدام كمادة خام رخيصة الثمن لصناعة مثبطات صديقة للبيئة. تم فحص الارتباط بين مستخلص تمر الغرس (GDE) وأيونات اليوديد لأول مرة لتحسين كفاءة تثبيط أنابيب الصلب API 5L X70 في 0.5 مول ل$^{-1}$ حامض الكبريتيك. وتمت دراسة التأثير الارتباطي لأيونات GDE واليوديد من خلال منحنيات الاستقطاب الديناميكي الفعال والتحليل الطيفي للمقاومة الكهروكيميائية ، والفحص المجهري الإلكتروني (SEM) والتحليل الطيفي للأشعة السينية المشتتة للطاقة (EDX). تبلغ كفاءة التثبيط 45.5٪ عند 2 جم ل$^{-1}$ GDE عند 20 درجة مئوية ، بينما تزداد إلى 97.9٪ عند إضافة 5×10^{-4} مول ل$^{-1}$ من يوديد البوتاسيوم عند 25 درجة مئوية. حيث تم الوصول إلى أنه يمكن الحصول على تثبيط كبير للتآكل بطريقة ارتباطية. يتبع نظام أيون GDE / يوديد متساوي امتصاص لانجمويير ، ويتضمن كلًا من الامتزاز الفيزيائي والامتزاز الكيميائي ويعمل كمثبط من النوع المختلط.

الكلمات المفتاحية: امتصاص كيميائي ؛ ثمار نخيل التمر مثبطات التآكل الخضراء. حمض الجالاكتورونيك. حامض الكبريتيك. تأثير تآزري